



Structural design, synthesis and substituent effect of hydrazone-*N*-acylhydrazones reveal potent immunomodulatory agents

Cássio S. Meira^a, José Maurício dos Santos Filho^b, Caroline C. Sousa^a, Pâmela S. Anjos^a, Jéssica V. Cerqueira^a, Humberto A. Dias Neto^b, Rafael G. da Silveira^c, Helena M. Russo^d, Jean-Luc Wolfender^d, Emerson F. Queiroz^d, Diogo R.M. Moreira^a, Milena B.P. Soares^{a,e,*}

^a FIOCRUZ, Instituto Gonçalo Moniz, 40296-710 Salvador, BA, Brazil

^b UFPE, Centro de Tecnologia e Geociências, Laboratory of Design and Synthesis Applied to Medicinal Chemistry-SintMed[®], CEP 50740-521 Recife, PE, Brazil

^c IFG, Campus Ceres, CEP 76300-000 Ceres, GO, Brazil

^d School of Pharmaceutical Sciences, EPGL, University of Geneva, University of Lausanne, CMU – Rue Michel-Servet 1, CH-1211 Geneva 4, Switzerland

^e Centro de Biotecnologia e Terapia Celular, Hospital São Rafael, 41253-190 Salvador, BA, Brazil

ARTICLE INFO

Article history:

Received 11 January 2018

Revised 16 February 2018

Accepted 23 February 2018

Available online 25 February 2018

Keywords:

Anti-inflammatory agents

Hydrazones

Methylation

Peritonitis

Substituent effects

ABSTRACT

4-(Nitrophenyl)hydrazone derivatives of *N*-acylhydrazone were synthesized and screened for suppress lymphocyte proliferation and nitrite inhibition in macrophages. Compared to an unsubstituted *N*-acylhydrazone, active compounds were identified within initial series when hydroxyl, chloride and nitro substituents were employed. Structure-activity relationship was further developed by varying the position of these substituents as well as attaching structurally-related substituents. Changing substituent position revealed a more promising compound series of anti-inflammatory agents. In contrast, an *N*-methyl group appended to the 4-(nitrophenyl)hydrazone moiety reduced activity. Anti-inflammatory activity of compounds is achieved by modulating IL-1 β secretion and prostaglandin E2 synthesis in macrophages and by inhibiting calcineurin phosphatase activity in lymphocytes. Compound **SintMed65** was advanced into an acute model of peritonitis in mice, where it inhibited the neutrophil infiltration after being orally administered. In summary, we demonstrated in great details the structural requirements and the underlying mechanism for anti-inflammatory activity of a new family of hydrazone-*N*-acylhydrazone, which may represent a valuable medicinal chemistry direction for the anti-inflammatory drug development in general.

© 2018 Elsevier Ltd. All rights reserved.

1. Introduction

Inflammatory responses are vital physiological processes in combating infections, as well as in recovering injury caused by foreign bodies and tissue damage; however, dysregulated or prolonged inflammatory responses can also induce tissue injury, giving rise to a number of inflammatory diseases.^{1,2} In response to an extracellular stimulus, macrophages can produce proinflammatory mediators, such as nitric oxide (NO) controlled by inducible nitric oxide synthase (iNOS), which is highly expressed upon activation of nuclear factor- κ B (NF- κ B) in response to many stimuli, including tumor necrosis factor alpha (TNF α) and interferon-gamma (IFN γ), among others.³ In addition, during an inflammatory response, activated macrophages overexpress cyclooxygenases

(COX1 and COX2), which are key enzymes responsible for the conversion of arachidonic acid into prostaglandin E2 (PGE2), a proinflammatory mediator involved in all processes leading to the classic signs of inflammation: redness, swelling and pain.⁴ Therefore, chemical inhibition of COX and iNOS can be useful in the management of inflammatory diseases.

The *N*-acylhydrazone group is a unique moiety very often employed into heterocyclic compounds drug design, which endow molecules with a better thermal stability as well as hydrolytic and chemical stability in comparison to amide group^{5–7}, in addition to the feasibility of varying chemical composition by substituent variation.^{8–11} Among the pharmacological effects of *N*-acylhydrazone-derived compounds, their anticancer and anti-inflammatory effects are well described.^{12,13} More specifically, *N*-acylhydrazone derivatives have been described as potential inhibitors of COX^{14–16}, iNOS¹⁷ and phosphodiesterases.^{18,19}

Lengthening the alkyl chain in the chemical structure of *N*-acylhydrazone-derived compounds has been identified as a strategy for

* Corresponding author at: FIOCRUZ, Instituto Gonçalo Moniz, CEP 40296-710 Salvador, BA, Brazil.

E-mail address: milena@bahia.fiocruz.br (M.B.P. Soares).

drug design and optimization. This can be achieved by inserting alkyl and alkene groups, such as the naturally-occurring cinnamic moiety. Hence, this strategy results in a plethora of diverse structures, along with interesting features, *i.e.*, planar structure, larger steric bulk and hydrophobic character.^{20–24} On the basis of these reports, the introduction of a side chain similar to the cinnamic moiety associated to the *N*-acylhydrazone functionality depicts a potential strategy for drug design. In an effort to develop novel anti-inflammatory agents, our research group envisaged the introduction of a 4-(nitrophenyl)hydrazone group on aryl-*N*-acylhydrazones, giving a class of hydrazone-*N*-acylhydrazones (HAH), where a nitro group was placed to enhance the electron-withdrawing characteristics (Fig. 1).^{25,26}

Once the 4-(nitrophenyl)hydrazone derivatives of *N*-acylhydrazone were designed, an efficient synthetic route was implemented on the grounds of the problem's retrosynthetic analysis (Scheme 1), leading to a series of novel compounds, which was studied by screening substituents attached to the aryl ring located near to the acyl group (Scheme 2). A set of *para*-substituents was selected by physical-chemical criteria: σ_p -Hammett constant, ranging from -0.83 for *N,N*-dimethylamino to $+0.78$ for nitro, lipophilicity and hydrogen bond acceptor/donor, allowing us to study the substituent effect on the activity. Encouraged by the initial screening, structure-activity relationship (SAR) for active compounds was further developed by varying the substituent position and employing structurally-related substituents. In addition to studying in great details the substituent effect of *N*-acylhydrazones for anti-inflammatory activity, we demonstrated the underlying mechanism of action as well as the efficacy of the most active compound, denoted here as **SintMed65**, in an acute peritonitis model of inflammation in mice.

2. Results and discussion

2.1. Chemistry

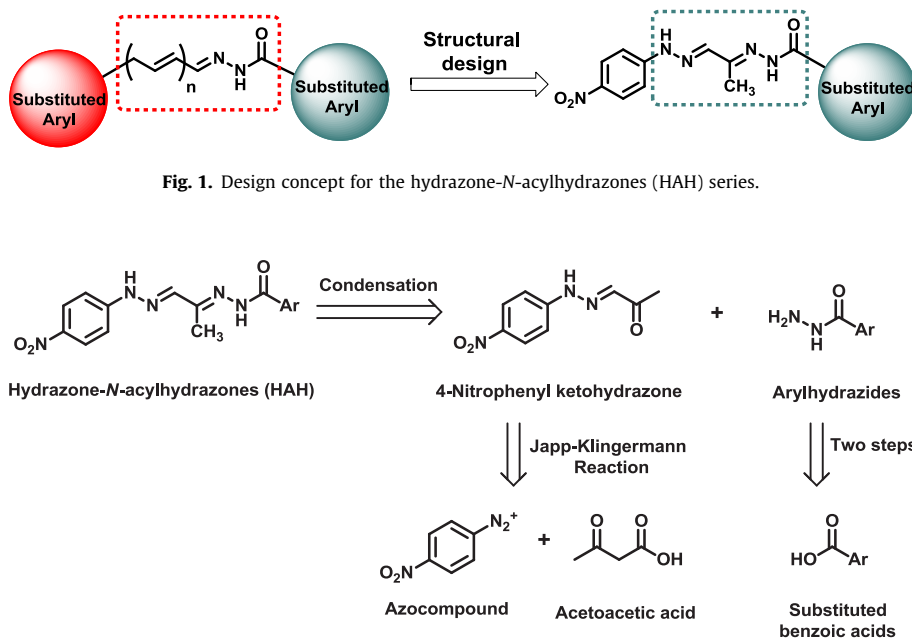
Once established the chemical template for the compounds to undergo a thorough anti-inflammatory investigation, our research group examined possible synthetic routes that could give access to them as expeditious as possible. The retrosynthetic analysis

depicted in Scheme 1 arises as an excellent option, since it leads to accessible starting materials, consists of well-established reactions and can be achieved using current methodologies developed at **SintMed**[®]. This approach starts with the disconnection of the *N*-acylhydrazone moiety, an almost conspicuous strategy, since it originates an arylhydrazide, the usual substrate for *N*-acylhydrazone formation, whose synthesis can easily be accomplished in two steps from commercial benzoic acids. Taking this path, the other constituent molecule is a 4-nitrophenyl ketohydrazone, whose preparation can be reached out by applying a Japp-Klingermann reaction involving 4-nitrophenyl diazonium salt and acetoacetic acid as reactants. Bottom line, all requirements to a fast and successful accomplishment of the planned work were completely fulfilled.

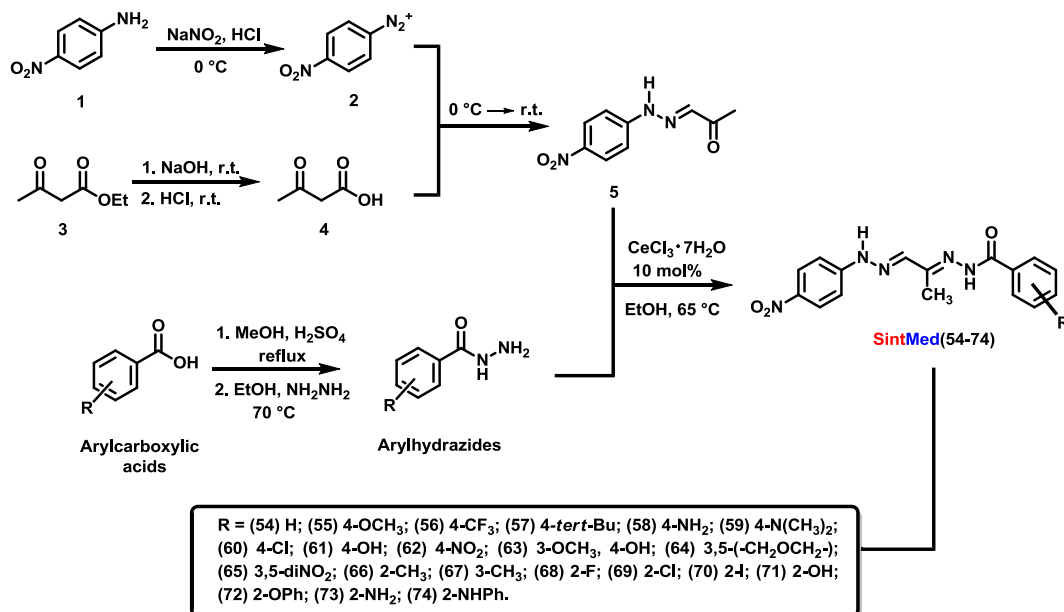
Based on this general strategy, the preparation of the targeted hydrazone-*N*-acylhydrazone compounds **SintMed(54–74)** followed the synthetic route shown in Scheme 2.

First, the diazotization of the 4-nitroaniline **1** provided the corresponding diazonium salt **2**, which reacted with the *in situ* generated acetoacetic acid **4** from the hydrolysis of its analogous ethyl acetoacetate **3**, as required by the Japp-Klingermann methodology. The 4-nitrophenyl ketohydrazone **5** was isolated in 95% yield. The arylhydrazides of interest could easily be prepared from commercial acids, whose refluxing Fisher esterification was carried out in methanol and sulfuric acid as catalyst. The methyl substituted aryl carboxylates were then converted into hydrazides by reaction with hydrazine hydrate at 70 °C, according to current methodologies in use at **SintMed**[®].^{8,9}

The condensation between the aryl hydrazides and the 4-nitrophenyl ketohydrazone **5** was accomplished under mild conditions in the presence of cerium(III) chloride heptahydrate as catalyst. This methodology was recently developed at **SintMed**[®],⁸ and is essential to the excellent outcomes observed for the HAH series, since the compound **5** is a vinylogous-like ketone, which does not withstand traditional acid conditions. Reacting both substrates at 65 °C in the presence of 10 mol% $\text{CeCl}_3 \cdot 7\text{H}_2\text{O}$ and ethanol, total conversion was observed in two hours without any decomposition or side products, as confirmed by TLC, and NMR analysis of crude products. More remarkable is the stereoselectivity observed from the NMR examination of the crude products, which indicates the



Scheme 1. Retrosynthetic strategy for the hydrazone-*N*-acylhydrazones (HAH) synthesis.



Scheme 2. Synthetic route for the hydrazone-*N*-acylhydrazones (HAH) preparation.

presence exclusively of the *E*-isomer. As previously demonstrated,^{8,9} the presence of isomeric mixtures of any nature leads to signal splitting on the ¹H NMR spectra, particularly easy to be observed for the hydrazone's amino hydrogen (–NH–N=), the hydrazone's imino (–N–N=CH–), the amido group (–CONH–), and the methyl linked to the imino portion (–N=CCH₃–) of the NAH. Most compounds of the series HAH exhibited only one signal for each of the mentioned groups, confirming the more stable *E*-isomer. Typical signals appear at ≈11.5 ppm (–NH–N=), ≈10.7 ppm (–CONH–), ≈7.74 ppm (–N–N=CH–), and ≈2.27 ppm (–N=CCH₃–) (See [Supporting Information](#)). Nevertheless, in some cases, *e.g.* *ortho*-substituted, and strong electron withdrawing groups bearing derivatives, the signal splitting can be observed. This particular behaviour was investigated by Barreiro et al.,^[27,28] who found out that it is due to the rotamery associated to specific structural features of such molecules, a conclusion in complete accordance with our previous reports.^{8,9} The expected stereochemical features of the HAH derivatives could be confirmed by crystallographic data collected for compound **SintMed65** (Fig. 2), which is an all-*E,E*-planar structure, held by the electronic delocalization through the molecule. This result also supports the rotameric nature of the signal splitting observed in some cases, including **SintMed65**.

Due to the outstanding biological results obtained with the HAH series, the key derivatives had their structures modified through

the nitrogen methylation of the hydrazone (–NH–N=) moiety, providing compounds **SintMed75–77**. In order to avoid a possible double methylation of the targeted molecules, a secondary synthetic route was applied, so that the 4-nitrophenyl ketohydrazone **5** was methylated in the presence of methyl iodide and potassium carbonate in acetone to give compound **6** in 94% yield, prior to undergoing the condensation with the appropriate hydrazides ([Scheme 3](#)).

2.2. Pharmacological evaluation

Nitric oxide production was estimated by measuring nitrite concentrations by the Griess method in the supernatants of J774 macrophages cultures 24 h after activation with LPS and IFN γ . The percentage of inhibition was determined at 20 μ M compound concentration as a primary screen, and compounds with% of inhibition >30% were considered active ([Table 1](#)). Assessment of cell viability was carried out by Alamarblue 72 h after drug exposure. Based on CC₅₀ values, compounds were not cytotoxic at 20 μ M.

Unsubstituted hydrazone-*N*-acylhydrazone **SintMed54** inhibited nitric oxide production. From the screening of 4-substituted HAH derivatives, in comparison to the unsubstituted compound, we observed that attachment of methoxy (**SintMed55**), trifluoromethyl (**SintMed56**), *tert*-butyl (**SintMed57**), amino (**SintMed58**), *N,N*-dimethylamino (**SintMed59**) or chlorine

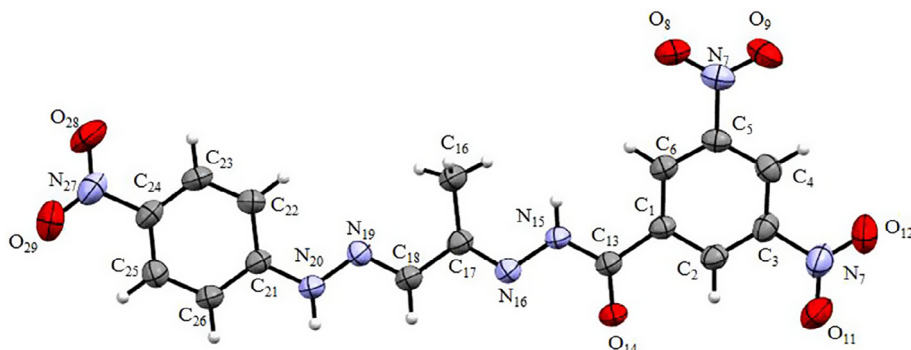
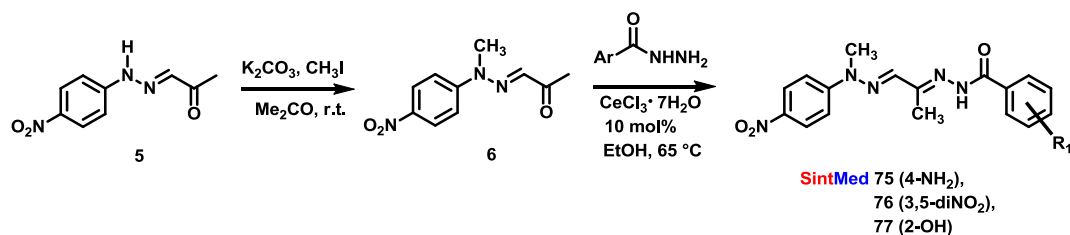


Fig. 2. ORTEP plot of X-ray crystal structure for **SINTMED65** compound. Atomic displacement parameters are shown at 50% probability level.



Scheme 3. Synthetic route for the *N*-methylated hydrazone-*N*-acylhydrazones.

(**SintMed60**) substituents diminished the activity, with a remarkably deleterious effect exerted by methoxy and *tert*-butyl groups, both bearing potent electron donating effect and no ability of donating or/and accepting hydrogen bonds. On the other hand, hydroxy (**SintMed61**) and nitro (**SintMed62**) substituents increased the activity, setting the general parameters ruling the influence of substituents on the biological activity. On the basis of these findings, we decided to expand the series of related compounds, exploiting diverse electronic properties, as well as ring positions' modifications.

The most promising compound from the initial series was the 4-hydroxyphenyl-derivative **SintMed61** (43.8 ± 1% of inhibition). Through the preparation and screening of the closely related analogues of this structure, **SintMed63** (3-methoxy-4-hydroxyphenyl substituted) and **SintMed64** (1,3-dioxole substituted), it became obvious that variation around the 4-hydroxy group is not tolerated, since the activity decreased for both associated compounds. In another attempt to improve activity, variation to the 2-position of the phenyl ring was then explored, affording 2-hydroxyphenyl (**SintMed71**) and 2-phenoxyphenyl (**SintMed72**) compounds. Changing the position of the hydroxy group did not abolish activity; in fact, compound **SintMed71** was found to be more potent than **SintMed61**, while the 2-phenoxy (**SintMed64**) compound was twice less active. Considering that both phenoxy and methoxy substituents decreased activity in comparison to the hydroxy-derived compounds, this suggests that a hydrogen bond donor substituent is required for activity.

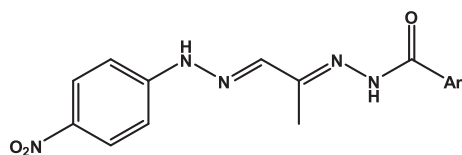
Due to the promising results when a substituent was attached at the 2-position, we carried out the screening of novel substituents. We observed that *o*-tolyl (**SintMed66**) or *m*-tolyl (**SintMed67**) compounds did not lead to active compounds. Albeit weak, the *o*-amino (**SintMed73**) compound inhibited in approximately twice the nitric oxide production in comparison to the *p*-amino (**SintMed58**) compound. Replacing the *o*-amino by an *o*-phenylamino (**SintMed74**) substituent, however, caused a marked loss in activity, indicating that limiting hydrogen-bond acceptor potential is deleterious for the activity. Screening halogen substituents led to a more interesting set of SAR information. Whereas 4-chloro derivative displayed weak effect, the 2-chloro derivative (**SintMed69**) was active. In order to exploit the effect of the electronic properties of different halogens, the 2-position was modified, introducing a fluorine (**SintMed68**), disclosing an inactive compound. On the other hand, the change of a 2-chloro for a 2-iodine substituent (**SintMed70**) produced a potent compound, demonstrating an inhibition value for nitric oxide production close to that of 2-hydroxyphenyl derivative **SintMed71**. These results suggest a crucial *ortho*-substituent effect for the activity of compounds. Extending our screening based on the observed result for the 4-nitrophenyl derivative **SintMed62** (39.1 ± 7% of inhibition), we designed compound **SintMed65**, whose structure bears two nitro groups at the positions 3 and 5 of the phenyl ring, a modification that disclosed the most potent derivative among all investigated molecules (73.5 ± 0.5% of nitric oxide inhibition). This evidenced the role of the nitro group in the activity.

As noted above with nitrophenyl compounds, electron-withdrawing substituents would not be indispensable for activity. When other electron-withdrawing substituents were attached, the resulting 4-trifluoromethylphenyl compound **SintMed56** and 2-fluorophenyl compound **SintMed68** were inactive. We first thought that a bioreduction of nitro into amino species may take place, being responsible for compound activity; however, a 4-amino compound lacks activity. One plausible explanation is that biological reduction of nitro group generates an *N*-(hydroxy)amino species; in agreement to this, we have the fact that hydroxy substituents confer activity for compounds. Considering the weak activity observed for the unsubstituted compound (which also contains a 4-nitro substituent at phenylhydrazone moiety), the position of nitro group is crucial for activity.

We next assessed the ability of compounds in inhibiting lymphocyte proliferation upon activation by concanavalin A (Con A). Compounds with IC₅₀ values <3.0 μM were considered active (Table 1). Unsubstituted compound **SintMed54** did not inhibit lymphocyte proliferation. From the screening of 4-substituted compounds, we observed that, in comparison to unsubstituted compound, attaching a hydroxy (**SintMed61**) or a nitro (**SintMed62**) substituent produced active compounds, while the attachment of other substituents did not lead to active compounds. Indeed, both 4-nitro (**SintMed62**) and 3,5-dinitro (**SintMed65**) compounds were the most active inhibitors of lymphocyte proliferation.

From the screening of 2-substituted compounds, we found that attaching a hydroxy (**SintMed71**) or iodine (**SintMed70**) substituents resulted in active compounds. In general, the most potent nitric oxide inhibitors also presented antiproliferative activity in lymphocytes. It was interesting to observe that, while *o*-hydroxyl (**SintMed71**) or *o*-iodine (**SintMed70**) derived compounds presented similar inhibitory activity in reducing nitric oxide production, hydroxyphenyl-derived compounds (**SintMed61**, **SintMed71**) were approximately twice more potent than iodine (**SintMed70**) compound. This indicates that hydrogen bond donor substituents have a superior effect on activity than halogen substituents.

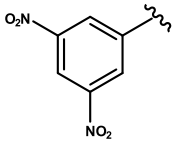
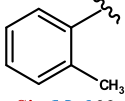
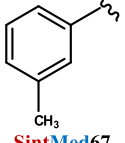

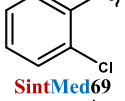
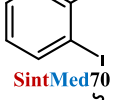
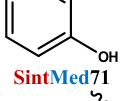
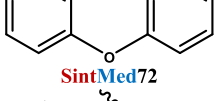
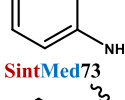
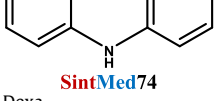
To gain insights regarding the 4-(nitrophenyl)hydrazone moiety for activity, we investigated the effect of *N*-methylation. To this end, we selected the two most active compounds (**SintMed65**, **SintMed71**) and one inactive compound (**SintMed58**) for modification. The synthesis of the respective *N*-methyl derived compounds (Scheme 3) was of high-yields, affording pure compounds after recrystallization in appropriate solvent. The results, summarized in Table 2, show that in contrast to non-methylated compounds, insertion of a methyl group did not increase nitric oxide inhibitory activity. Regarding IC₅₀ for lymphocyte proliferation, we observed a 2- to 3-fold reduction in the activity. While this result indicates the importance of a free hydrazone group for activity, it also points out that the aryl-acylhydrazone moiety is sensitive for molecular modification, possible because it represents a pharmacophoric group.

Table 1*In vitro* screening on cell viability, lymphocyte proliferation and nitric oxide inhibition.

Ar/Codes	Cell viability ^a (CC ₅₀ ± S.E.M., μM)	Inhibition (%) of nitrite production at 20 μM (Mean ± S.D.) ^b	Lymphocyte proliferation ^c (IC ₅₀ ± S.E.M., μM)
 SintMed54	>100	31.4 ± 2	>12
 SintMed55	>100	7.5 ± 0.2	>12
 SintMed56	78.7 ± 6.2	18.7 ± 5	>12
 SintMed57	>100	4.8 ± 3	>12
 SintMed58	75 ± 8	12.8 ± 1	>12
 SintMed59	>100	25.6 ± 3	>12
 SintMed60	63.9 ± 5.0	23.0 ± 3	4.2 ± 0.2
 SintMed61	51 ± 1.5	43.8 ± 1	1.51 ± 0.007
 SintMed62	>100	39.1 ± 7	0.98 ± 0.03
 SintMed63	>100	6.6 ± 0.9	5.1 ± 0.9
 SintMed64	>100	23.2 ± 5	>12

(continued on next page)

Table 1 (continued)

Ar/Codes	Cell viability ^a (CC ₅₀ ± S.E.M., μM)	Inhibition (%) of nitrite production at 20 μM (Mean ± S.D.) ^b	Lymphocyte proliferation ^c (IC ₅₀ ± S.E.M., μM)
 SintMed65	17.8 ± 3.1	75.3 ± 0.5	0.27 ± 0.02
 SintMed66	>100	21.9 ± 2	6.0 ± 0.5
 SintMed67	>100	9.3 ± 0.9	>12
 SintMed68	>100	5.3 ± 0.1	>12
 SintMed69	>100	39.4 ± 1.2	>12
 SintMed70	40 ± 4.1	56.8 ± 2	2.98 ± 0.5
 SintMed71	29.5 ± 1.3	59.7 ± 4	1.64 ± 0.01
 SintMed72	>100	5.5 ± 3	>12
 SintMed73	29.8 ± 2.9	39.3 ± 0.5	4.9 ± 0.5
 SintMed74	>100	14.1 ± 0.2	N.D.
Dexa	91.1 ± 1.9	69.8 ± 2	0.001 ± 0.0005
GV	4.1 ± 0.05	–	–

^a J774 cell viability assessed by Alamarblue 72 h after drug incubation and expressed as CC₅₀.

^b Percent inhibition determined 24 h after incubation with compounds and LPS plus IFN-γ.

^c Proliferation of lymphocytes induced by concanavalin A (con A), determined by thymidine uptake 72 h after drug incubation and expressed as IC₅₀. Values represents the mean ± S.E.M. and were calculated from three independent experiments performed. Abbreviations: IC₅₀ = inhibitory concentration at 50%; CC₅₀ = cytotoxic concentration at 50%; Dexa = Dexamethasone; GV = gentian violet; S.E.M. = standard error of mean.

SintMed65 was the most active compound in inhibiting nitric oxide production by macrophages, as well as in inhibiting lymphocyte proliferation, and therefore it was selected to evaluate its mechanisms of action. To exclude that **SintMed65** effects were related to cytotoxic effects, in the next experiments we evaluated its immunomodulatory effect in concentrations up to 12 μM, that showed no toxicity in macrophages and lymphocytes cells (data not shown).

In the presence of **SintMed65** (2.5–10 μM), a significant and concentration-dependent inhibition of nitric oxide production was observed (Fig. 3A). Furthermore, we evaluated its effect on the synthesis of proinflammatory cytokines TNFα, IL-1β and IL-6 (Fig. 3). A significant and concentration-dependent inhibition of IL-1β and IL-6 was observed, while for TNFα, **SintMed65** compound only inhibited its secretion when added at 10 μM. In various cell types, IL-1β is a potent inducer of COX2 expression, an

Table 2
Comparison of activity between HAH and its *N*-methyl derivatives.

N-methylation

Ar/Codes	Cell viability ^a (CC ₅₀ ± S.E.M., μM)	Inhibition (%) of nitrite production at 20 μM (Mean ± S.D.) ^b	Lymphocyte proliferation ^c (IC ₅₀ ± S.E.M., μM)
	51.7 ± 4.0	3.6 ± 2	>12
	39.0 ± 3.1	51.0 ± 2.5	1.11 ± 0.07
	31.5 ± 0.9	41.0 ± 2	3.12 ± 0.4

^{a,b,c} See footnote in Table 1.

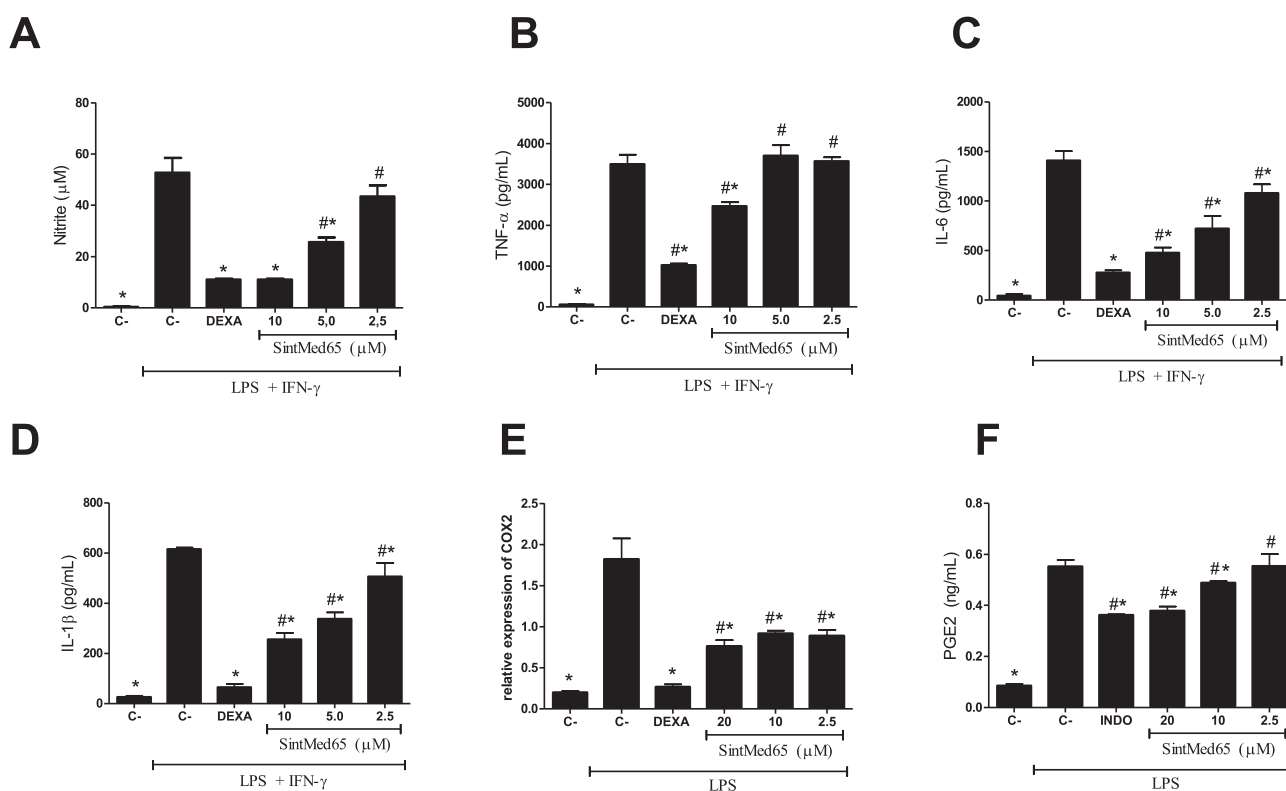


Fig. 3. Immunomodulatory effects of *N*-acylhydrazone **SintMed65** on pro-inflammatory mediators. (A–D) Peritoneal macrophages of BALB/c mouse were stimulated *in vitro* with LPS (0.5 μg/mL) and IFN-γ (10 ng/mL) and treated with different concentrations of **SintMed65** (10, 5 and 2.5 μM) or dexamethasone (DEXA; 10 μM). Supernatants were collected for nitrite quantification by Griess method and cytokines by ELISA. (E and F) J774 macrophages were stimulated with LPS (0.1 μg/mL) and treated with different concentrations of **SintMed65** (10, 5 and 2.5 μM) or DEXA (10 μM) or Indomethacin (INDO; 20 μM). PGE2 determination was done by enzyme immunoassay (EIA) and COX2 gene expression by qPCR 24 h after challenge. Values represent the mean ± S.E.M. of one of two experiments performed. One-way ANOVA and Newman-Keuls test: **P* < 0.05 compared to stimulated and untreated cells; #*P* < 0.05 compared to dexamethasone-treated cells or indomethacin-treated cells.

enzyme that controls the biosynthesis of PGE2, an important inflammatory mediator.^{29,30} Therefore, considering that IL-1β secretion was inhibited by **SintMed65**, we decided to investigate this pathway. PGE2 production and COX2 gene transcription

were evaluated in LPS-activated J774 cells, according to standard protocols.³¹ As observed in Fig. 3, **SintMed65** reduced COX2 expression and PGE2 biosynthesis in a concentration-dependent manner.

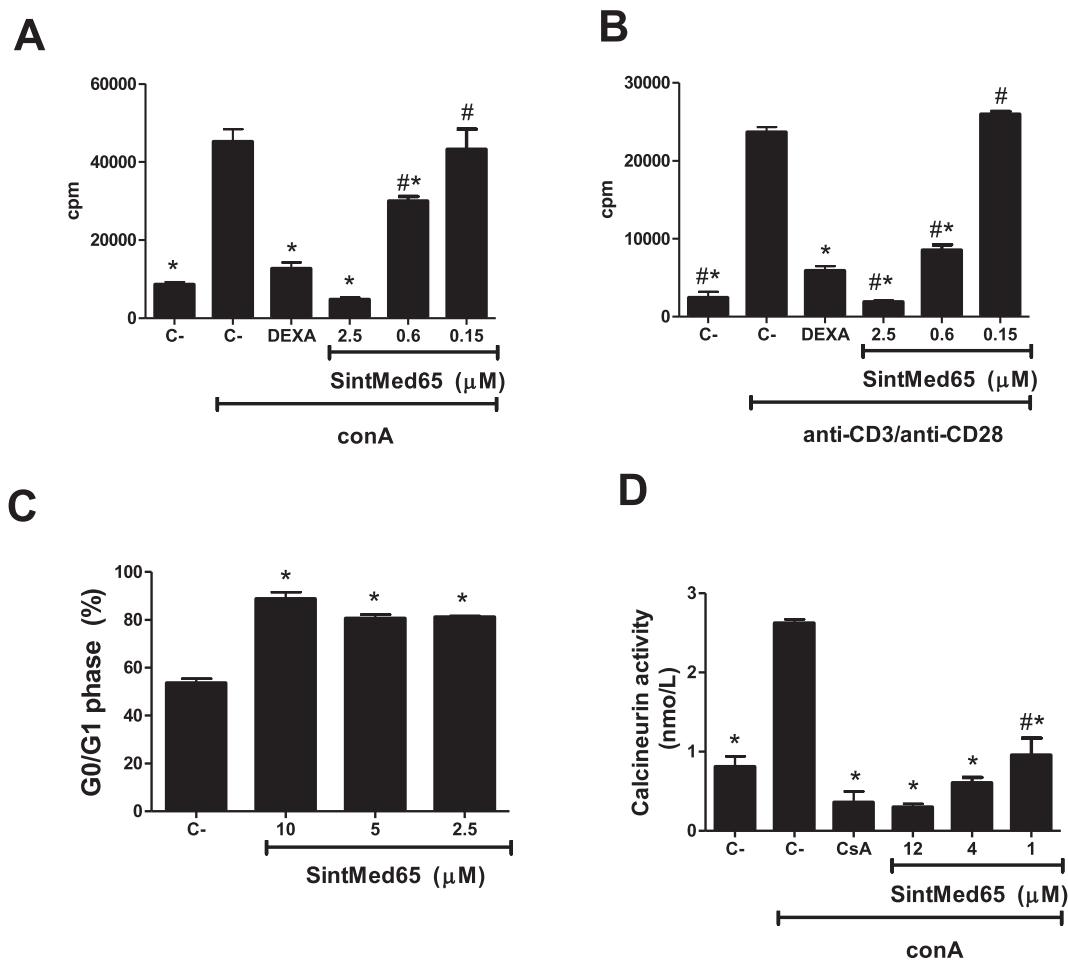


Fig. 4. N-acylhydrazone **SintMed65** inhibits lymphocyte proliferation by arresting cell cycle and inhibiting calcineurin activity. Proliferation of lymphocytes stimulated with Con A (panel A) or anti-CD3/anti-CD28 beads (panel B). Proliferation rates were assessed through ^3H -thymidine incorporation. Lymphocytes stimulated with conA, incubated for 48 h, stained for PI (2 $\mu\text{g}/\text{ml}$) and analyzed by flow cytometry (panel C). Cellular calcineurin activity in lymphocytes determined by colorimetric assay (panel D). Error bars represent the mean \pm S.E.M. Dexa = Dexamethasone, 1.0 μM . CsA = Cyclosporin A, 12 μM . One-way ANOVA and Newman-Keuls test: * $P < 0.05$ compared to stimulated and untreated cells; # $P < 0.05$ compared to dexamethasone-treated cells or cyclosporin A-treated cells.

Next, we evaluated the underlying effects of **SintMed65** compound on lymphocyte proliferation induced by Con A or anti-CD3/anti-CD28 (Fig. 4).

In both assays, **SintMed65** exhibited a significant and concentration-dependent suppression of lymphoproliferation. As a potential immunotherapeutic agent, it was also important to determine the effect of **SintMed65** on cytokine secretion. To this end, cytokine production by splenocytes stimulated with Con A and treated with **SintMed65** was investigated (Fig. 5). Compared to untreated and stimulated cultures, treatment with **SintMed65** decreased the secretion of IL-2, IL-4, IL-10, IL-17A and IFN- γ in a concentration-dependent manner. Under the same conditions, dexamethasone also promoted a significant decrease in cytokine production (Fig. 5).

We further investigated whether **SintMed65** compound inhibits lymphocyte proliferation by blocking cell cycle progression. As observed in Fig. 5C, treatment with **SintMed65** induced cell cycle arrest on G0/G1 phase in comparison to untreated and stimulated control. TCR activation increases the intracellular calcium concentration on T lymphocytes, activating calcineurin, a phosphatase that dephosphorylates NFAT transcription factor.^{32,33} Notably, NFAT is involved in the transcriptional activation of genes encoding several cytokines important for lymphocyte expansion and differentiation.³⁴ We found that **SintMed65** treatment significantly reduced cellular calcineurin phosphate activity in Con A-activated lymphocytes after 72 h of culture (Fig. 5D). These data

suggest that **SintMed65** effect on lymphocyte proliferation is likely due to its cell cycle blockage and calcineurin inhibition.

Finally, we evaluated **SintMed65** compound in an *in vivo* model of carrageenan-induced mouse peritonitis. Indomethacin, a COX inhibitor, was used as reference drug. In comparison to untreated group (vehicle), pre-treatment for 1 h of **SintMed65** at 80 and 20 mg/kg by oral route caused a reduction in the number of neutrophils of 30.6 and 21.4%, respectively (Fig. 6). Under the same conditions, treatment with indomethacin (80 mg/kg) caused a reduction of 35.9%.

3. Conclusions

We demonstrated that the structural design of 4-(nitrophenyl) hydrazone derivatives of N-acylhydrazone led to a new family of potent anti-inflammatory and immunosuppressor agents. By investigating a number of substituents, as well as structural modification, we observed that activity was affected by the nature and position of the attached substituent, revealing a key role of substituent effect for activity. We have found that this family of compounds inhibits nitric oxide production by activated macrophages, which is achieved by suppressing IL-1 β secretion, with subsequent reduction in COX2 expression and PGE2 biosynthesis. Moreover, these hydrazone-N-acylhydrazones were able to inhibit lymphocyte proliferation and cytokine production, showing a potent immunomodulatory action. Furthermore, oral administration of

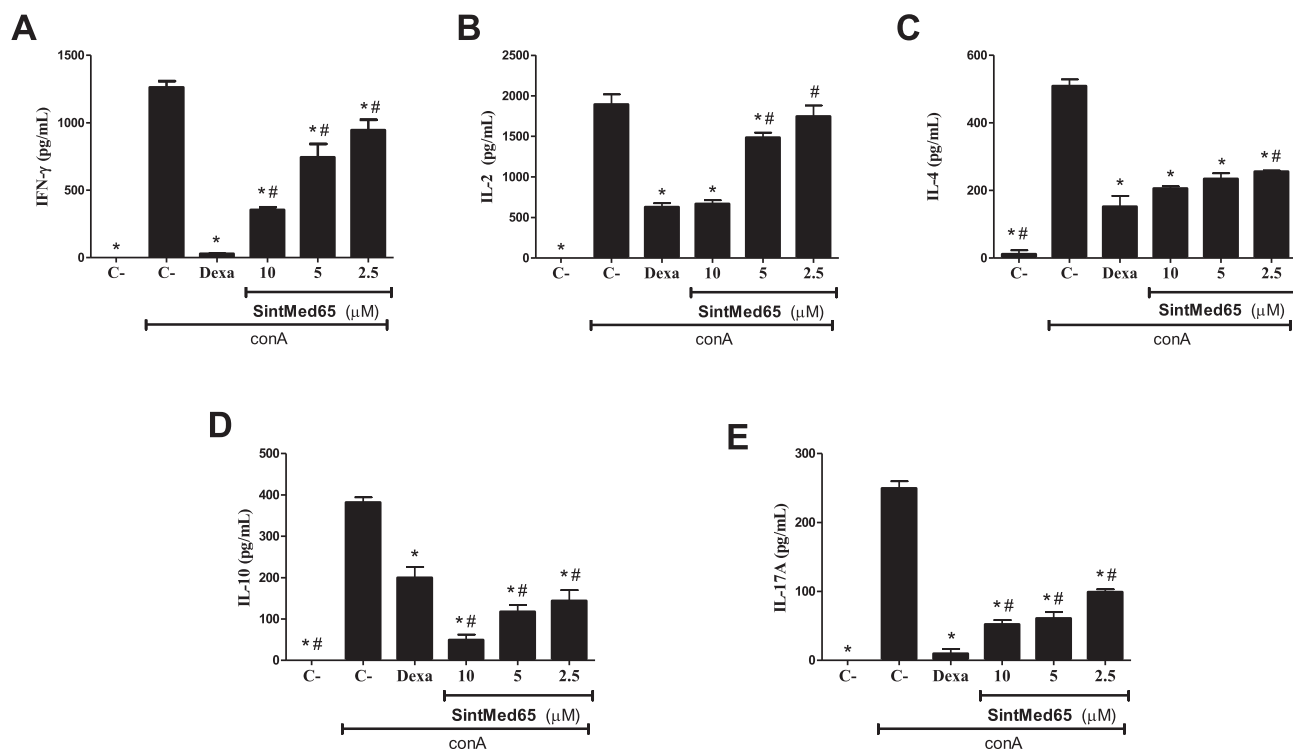


Fig. 5. N-acylhydrazone **SintMed65** modulates cytokine production by activated lymphocytes. Lymphocytes were stimulated with con A and treated with different concentrations of **SintMed65** (10, 5 and 2.5 μM) or dexamethasone (Dexa; 1 μM). Cytokines were determined by ELISA in the supernatant collected 48 h after stimulus. Dexa = Dexamethasone at 10 μM , except for IL-2, which it was used at 1.0 μM . Values represent the mean \pm S.E.M. of one of two experiments performed. One-way ANOVA and Newman-Keuls test: * $P < 0.05$ compared to stimulated and untreated cells; # $P < 0.05$ compared to dexamethasone-treated cells.

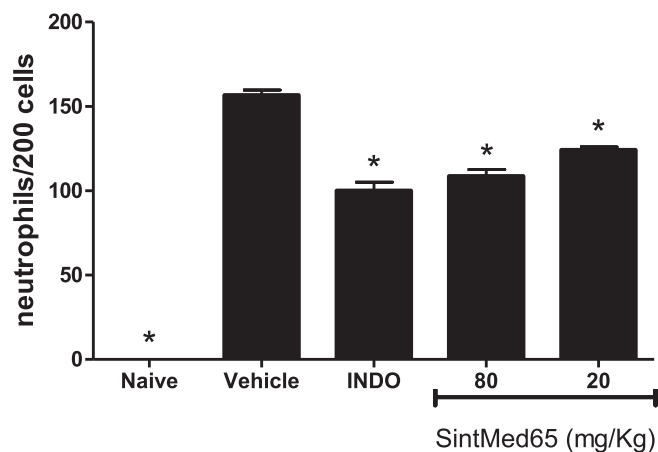


Fig. 6. **SintMed65** is an oral anti-inflammatory agent in a model of peritonitis. Male BALB/c mice ($n = 6/\text{group}$) were treated orally by gavage 1 h before challenge with carrageenan (1%; v/v). Indomethacin (INDO) at 80 mg/kg was used as reference anti-inflammatory by intraperitoneal route. Exudate was collected 4 h after the injection of carrageenan. Values represent the mean \pm S.E.M. of one experiment of two experiments performed. One-way ANOVA and Newman-Keuls test: * $P < 0.05$ compared to vehicle group; # $P < 0.05$ compared to indomethacin group.

SintMed65 compound significantly decreased inflammatory cell migration in a peritonitis model induced by carrageenan.

4. Materials and methods

4.1. Chemistry

4.1.1. General methods

All solvents, carboxylic acids, and other reactants were purchased from Merck, Sigma-Aldrich and Vetec, and were used without further purification. Esters were obtained by Fischer

esterification of commercial carboxylic acids. Hydrazide derivatives were synthesised from the corresponding carboxylic esters by reaction with hydrazine hydrate, following literature methods currently applied in our laboratory.^{8,9} Reactions progress were monitored by thin layer chromatography (TLC), performed onto glass-backed plates of silica gel 60 F254 with gypsum, and all compounds were detected by ultraviolet light (254 nm) as well as by iodine vapour. Melting points were determined with a Gehaka PF1500 capillary apparatus, and are uncorrected. NMR spectra were recorded at 400 MHz for hydrogen and 100 MHz for carbon nuclei, using a Varian UNMRS 400 spectrometer, as well as at 300 MHz for hydrogen and 75 MHz for carbon nuclei, using a Varian Unitplus 300, in $\text{DMSO}-d_6$ with chemical shift values (δ) in parts per million (ppm) and coupling constants (J) in Hertz (Hz), all measured at 25 $^\circ\text{C}$. Structural assignments for known compounds were made by comparison of recorded spectra with literature data experiments, while new compounds were assigned by 2D experiments, and described according to the IUPAC numbering rules. IR spectra were recorded on a Tensor27 FTIR spectrometer from Bruker with the samples being analyzed as KBr pellets. High resolution mass spectrometry (HRMS) analysis of the pure compounds was performed with an UHPLC-ESI-HRMS on a Micromass LCT Premier time-of-flight mass spectrometer from Waters with an electrospray ionization (ESI) interface (Waters, Milford, MA, USA) equipped with an electrospray interface and coupled to an Acquity UHPLC system (Waters, Milford MA, USA). UHPLC-ESI-HRMS analysis was performed using the following parameters: ESI used capillary voltage 2800 V, cone voltage 40 V, MCP detector voltage 2400 V, source temperature 120 $^\circ\text{C}$, desolvation temperature 300 $^\circ\text{C}$, cone gas flow 20 L/h, and desolvation gas flow 800 L/h. Detection was performed in positive ion mode (PI) with a m/z range of 100–1300 Da and a scan time of 0.5 s in the W-mode. The MS was calibrated using sodium formate, and leucine encephalin (Sigma-Aldrich, Steinheim, Germany) was used as an internal

reference at 2 µg/mL and infused through a Lock Spray™ probe at a flow rate of 10 µL/min with the help of a second LC pump. The separation was performed on an Acquity BEH C₁₈ UPLC column (1.7 µm, 50 × 2.1 mm i.d.; Waters, Milford, MA, USA) using a linear gradient, solvent system: A) 0.1% formic acid-water, B) 0.1% formic acid-acetonitrile; gradient: 5–36% B in 1 min, then 36% B to 36% B in 2 min, 36% B to 95% B in 1.5 min; flow rate 1.1 mL/min. The temperature was set at 40 °C. The injected volume was kept constant (1 µL; solution at the concentration of 0.5 mg/mL). Elemental analyses were performed in a Perkin Elmer2400 Series L elemental analyzer.

4.1.2. Synthesis of α -oxopropane-4-nitrophenylhydrazone (5)

In a 100 mL round bottom flask, a solution 0.8028 g of potassium hydroxide 85% was prepared in 22 mL of water at room temperature, followed by the addition of 1.20 mL (10.12 mmol) of ethyl acetoacetate **3**, and the mixture was kept stirring for 24 h. After this time, the solution was chilled using an ice/salt bath until the temperature was below 5 °C. In a second flask, a suspension of 1.4000 g (10.12 mmol) of *p*-nitroaniline **1** in 10.0 mL water was placed in an ice/salt bath until the temperature reached 5 °C. A cold solution of 4.0 mL of concentrated hydrochloric acid and 4.0 mL water was poured to the suspension, dissolving the solid almost completely. Under stirring, a cold solution of 0.8392 g (12.16 mmol) of sodium nitrite in 2.0 mL water was added dropwise to the acid solution of *p*-nitroaniline. The rate of addition was regulated, so that the reaction's temperature did not rise above 5 °C. The resulting diazonium salt solution was kept under such conditions, while the initial solution of potassium acetoacetate was acidified with a mixture of 1.0 mL of concentrated hydrochloric acid and 3.0 mL water at 0 °C, followed by the addition of 1.6630 g (20.20 mmol) of sodium acetate. Finally, the cold solution of the acetoacetic acid was added in portions to the solution of diazonium salt under vigorous stirring, observing the immediate formation of a yellow precipitate. Once the addition was finished, the reaction mixture was stirred for more 30 min at 0 °C, and the ice bath was removed, allowing the medium to reach the room temperature. After 30 min, 20 mL water was poured into the reaction mixture, which was refluxed at 50 °C for 2 h. After cooling to room temperature, the mixture was allowed to stand in the refrigerator overnight prior to vacuum filtration and washing with cold water. Compound **5** was obtained as yellow powder. Yield 95%; mp 221.9–222.7 °C; R_f 0.21 (AcOEt/Hexanes 3:7); IR (KBr, ν_{\max} cm⁻¹): 3252, 3150 (N–H), 3078 (Ar C–H), 2924 (C–H), 1675 (C=O), 1587 (C=N); ¹H NMR (400 MHz, DMSO-*d*₆, δ ppm): 8.34 (d, 2H, ³J = 9.6 Hz, 4-NO₂Ph H-3,5), 7.48 (s, 1H, N=CH), 7.43 (d, 2H, ³J = 8.8 Hz, 4-NO₂Ph H-2,6), 2.50 (s, 3H, CH₃); ¹³C NMR (100 MHz, DMSO-*d*₆, δ ppm): 196.7 (1C, C=O), 148.9 (1C, 4-NO₂Ph C-4), 140.7 (1C, 4-NO₂Ph C-1), 138.6 (1C, N=CH), 125.9 (2C, 4-NO₂Ph C-3,5), 113.1 (2C, 4-NO₂Ph C-2,6), 24.3 (1C, CH₃).

4.1.3. General procedure for the synthesis of hydrazone-*N*-acylhydrazones SintMed(54–74)

To a stirred suspension of α -oxopropane-4-nitrophenylhydrazone (**5**) (0.48 mmol) and the appropriate hydrazide (0.48 mmol) in 4.0 mL of ethanol, cerium (III) chloride heptahydrate (10 mol%) was added and the reaction mixture was stirred at 65 °C during 1–3 h. Reaction's completion was monitored by TLC, using appropriate eluent system. Once concluded, the heating was put away, and the reaction mixture was allowed to reach room temperature, giving yellow to orange precipitates. After cooling, the solids were filtered off under vacuum, and washed with cold ethanol. ¹H NMR analysis of all products confirmed their purity. Recrystallization from ethanol afforded the samples for biological purposes, which were dried in an Abderhalden's apparatus to remove traces of

solvent. Yields, melting points, spectroscopic and spectrometric data are listed below for each new compound.

4.1.3.1. *N'*-[(1*E*)-3-(4-nitrophenylhydrazono)]-(2*E*)-propan-2-ylidenebenzohydrazide (SintMed54). Yellow solid, yield 90%; mp 294.5–295.9 °C (dec); R_f 0.60 (AcOEt); IR (KBr, ν_{\max} cm⁻¹): 3374, 3222, 3197, 3142 (N–H), 3063, 3026 (C–H Ar), 2970, 2922 (C–H), 1654 (s, C=O), 1610 (C=C), 1597 (C=N); ¹H NMR (400 MHz, DMSO-*d*₆, δ ppm): 11.5 (s, 1H, NH), 10.8 (s, 1H, CONH), 8.15 (d, 2H, ³J = 8.8 Hz, 4-NO₂Ph H-3,5), 7.86 (d, 2H, ³J = 6.0 Hz, Ph H-2,6), 7.74 (s, 1H, N=CH), 7.57 (d, 1H, ³J = 7.2 Hz, Ph H-4), 7.50 (t, 2H, ³J = 7.2 Hz, Ph H-3,5), 7.16 (d, 2H, ³J = 8.8 Hz, 4-NO₂Ph H-3,5), 2.27 (s, 3H, CH₃); ¹³C NMR (100 MHz, DMSO-*d*₆, δ ppm): 163.9 (1C, C=O), 152.1 (1C, CH₃C=N), 149.9 (1C, 4-NO₂Ph C-1), 142.1 (1C, N=CH), 139.0 (1C, 4-NO₂Ph C-4), 133.6 (1C, Ph C-1), 131.5 (1C, Ph C-4), 128.1 (4C, Ph C-2,3,5,6), 126.0 (2C, 4-NO₂Ph C-3,5), 111.6 (2C, 4-NO₂Ph C-2,6), 11.2 (1C, CH₃); UHPLC-TOF-MS for C₁₆H₁₅N₅O₃ calcd (found)/Error: 324.1094 (324.1097 [M–H]⁻)/–0.9 ppm; 326.1254 (326.1253, [M+H]⁺)/0.3 ppm.

4.1.3.2. *N'*-[(1*E*)-3-(4-nitrophenylhydrazono)]-(2*E*)-propan-2-ylidene-4-methoxybenzohydrazide (SintMed55). Yellow solid, yield 84%; mp 291.9–292.4 °C; R_f 0.50 (AcOEt); IR (KBr, ν_{\max} cm⁻¹): 3226, 3199 (N–H), 3068, 3024 (C–H Ar), 2965 2932 (C–H), 1680 (C=O), 1607 (C=C), 1569 (C=N); ¹H NMR (400 MHz, DMSO-*d*₆, δ ppm): 11.5 (s, 1H, NH), 10.7 (s, 1H, CONH), 8.15 (d, 2H, ³J = 8.8 Hz, 4-NO₂Ph H-3,5), 7.87 (d, 2H, ³J = 8.4 Hz, 4-CH₃Oph H-2,6), 7.74 (s, 1H, N=CH), 7.16 (d, 2H, ³J = 8.8 Hz, 4-NO₂Ph H-2,6), 7.03 (d, 2H, ³J = 8.0 Hz, 4-CH₃Oph H-3,5), 3.83 (s, 3H, OCH₃), 2.27 (s, 3H, CH₃); ¹³C NMR (100 MHz, DMSO-*d*₆, δ ppm): 163.5 (1C, C=O), 162.0 (1C, 4-CH₃Oph C-4), 152.3 (1C, CH₃C=N), 149.9 (1C, 4-NO₂Ph C-1), 142.3 (1C, N=CH), 138.9 (1C, 4-NO₂Ph C-4), 130.1 (2C, 4-CH₃Oph C-2,6), 126.0 (2C, 4-NO₂Ph C-3,5), 125.5 (1C, 4-CH₃Oph C-1), 113.4 (2C, 4-CH₃Oph C-3,5), 111.5 (2C, 4-NO₂Ph C-2,6), 55.3 (1C, OCH₃), 11.1 (1C, CH₃); UHPLC-TOF-MS for C₁₇H₁₇N₅O₄ calcd (found)/Error: 354.1212 (354.1202, [M–H]⁻)/2.8 ppm; 356.1371 (356.1359, [M+H]⁺)/3.4 ppm.

4.1.3.3. *N'*-[(1*E*)-3-(4-nitrophenylhydrazono)]-(2*E*)-propan-2-ylidene-4-trifluoromethylbenzohydrazide (SintMed56). Orange solid, yield 82%; mp 303.4–304.2 °C (dec); R_f 0.48 (AcOEt); IR (KBr, ν_{\max} cm⁻¹): 3298, 3234 (N–H), 3028 (C–H Ar), 2968 (C–H), 1640 (C=O), 1599 (C=C), 1566 (C=N); ¹H NMR (400 MHz, DMSO-*d*₆, δ ppm): 11.5 and 11.3 (s, 1H, NH), 11.3 and 11.0 (s, 1H, CONH), 8.15 (d, 2H, ³J = 9.2 Hz, 4-NO₂Ph H-3,5), 8.04 (br s, 2H, 4-CF₃Ph H-3,5), 7.87 (d, 2H, ³J = 6.8 Hz, 4-CF₃Ph H-2,6), 7.76 (s, 1H, N=CH), 7.17 (d, 2H, ³J = 6.4 Hz, 4-NO₂Ph H-2,6), 2.28 (s, 3H, CH₃); ¹³C NMR (100 MHz, DMSO-*d*₆, δ ppm): 163.0 (1C, C=O), 154.1 (1C, CH₃C=N), 149.8 (1C, 4-NO₂Ph C-1), 141.9 (1C, N=CH), 139.1 (1C, 4-NO₂Ph C-4), 137.6 (1C, 4-CF₃Ph C-4), 128.9 (2C, 4-CF₃Ph C-3,5), 126.0 (2C, 4-NO₂Ph C-3,5), 125.2 (2C, 4-CF₃Ph C-2,6), 122.5 (1C, 4-CF₃Ph C-1), 111.6 (2C, 4-NO₂Ph C-2,6), 11.4 (1C, CH₃); ¹⁹F NMR (376 MHz, DMSO-*d*₆, δ ppm): –61.4 (s, 3F, CF₃); UHPLC-TOF-MS for calcd (found)/Error: 392.0985 (392.0970, [M–H]⁻)/3.8 ppm; 394.1149 (394.1127, [M+H]⁺)/5.6 ppm.

4.1.3.4. *N'*-[(1*E*)-3-(4-nitrophenylhydrazono)]-(2*E*)-propan-2-ylidene-4-*tert*-butylbenzohydrazide (SintMed57). Yellow solid, yield 93%; mp 300.3–301.4 °C; R_f 0.45 (AcOEt); IR (KBr, ν_{\max} cm⁻¹): 3226, 3143 (N–H), 3067 (C–H Ar), 2964, 2869 (C–H), 1665 (C=O), 1597 (C=C), 1571 (C=N); ¹H NMR (400 MHz, DMSO-*d*₆, δ ppm): 11.5 (s, 1H, NH), 10.8 (s, 1H, CONH), 8.15 (d, 2H, ³J = 8.8 Hz, 4-NO₂Ph H-3,5), 7.79 (d, 2H, ³J = 8.0 Hz, 4-^tBuPh H-2,6), 7.74 (s, 1H, N=CH), 7.51 (d, 2H, ³J = 8.4 Hz, 4-^tBuPh H-3,5), 7.16 (d, 2H, ³J = 8.8 Hz, 4-NO₂Ph H-2,6), 2.26 (s, 3H, CH₃), 1.31 (s, 9H, ^tBu); ¹³C NMR (100 MHz, DMSO-*d*₆, δ ppm): 163.9 (1C, C=O),

154.4 (1C, 4-^tBuPh C-4), 152.8 (1C, CH₃C=N), 149.9 (1C, 4-NO₂Ph C-1), 142.2 (1C, N=CH), 138.9 (1C, 4-NO₂Ph C-4), 130.9 (1C, 4-^tBuPh C-1), 127.9 (2C, 4-^tBuPh C-2,6), 126.0 (2C, 4-NO₂Ph C-3,5), 124.9 (2C, 4-^tBuPh C-3,5), 111.6 (2C, 4-NO₂Ph C-2,6), 34.6 (1C, C(CH₃)₃), 30.8 (3C, C(CH₃)₃), 11.1 (1C, CH₃); UHPLC-TOF-MS for C₂₀H₂₃N₅O₃ calcd (found)/Error: 380.1700 (380.1723, [M-H]⁻)/-6.0 ppm; 382.1877 (382.1879, [M+H]⁺)/-0.5 ppm.

4.1.3.5. *N'-[(1E)-3-(4-nitrophenylhydrazono)]-(2E)-propan-2-ylidene-4-aminobenzohydrazide (SintMed58)*. Yellow solid, yield 90%; mp 302.1–302.7 °C (dec); R_f 0.35 (AcOEt); IR (KBr, ν_{max} cm⁻¹): 3474, 3381, 3223, 3192, 3139 (N-H), 3064, 3026 (C-H Ar), 1648 (s, C=O), 1599 (C=C), 1568 (C=N); ¹H NMR (400 MHz, DMSO-*d*₆, δ ppm): 11.4 (s, 1H, NH), 10.3 (s, 1H, CONH), 8.14 (d, 2H, ³J = 9.2 Hz, 4-NO₂Ph H-3,5), 7.74 (s, 1H, N=CH), 7.66 (d, 2H, ³J = 8.0 Hz, 4-NH₂Ph H-2,6), 7.15 (d, 2H, ³J = 9.2 Hz, 4-NO₂Ph H-2,6), 6.60 (d, 2H, ³J = 8.8 Hz, 4-NH₂Ph H-3,5), 5.79 (s, 2H, NH₂), 2.25 (s, 3H, CH₃); ¹³C NMR (100 MHz, DMSO-*d*₆, δ ppm): 163.8 (1C, C=O), 152.3 (1C, 4-NH₂Ph C-4), 150.6 (1C, CH₃C=N), 150.0 (1C, 4-NO₂Ph C-1), 142.6 (1C, N=CH), 138.8 (1C, 4-NO₂Ph C-4), 130.0 (2C, 4-NH₂Ph C-2,6), 126.0 (2C, 4-NO₂Ph C-3,5), 119.4 (1C, 4-NH₂Ph C-1), 112.4 (2C, 4-NH₂Ph C-3,5), 111.5 (2C, 4-NO₂Ph C-2,6), 10.9 (1C, CH₃); UHPLC-TOF-MS for C₁₆H₁₆N₆O₃ calcd (found)/Error: 339.1256 (339.1206, [M-H]⁻)/14.7 ppm; 341.1346 (341.1362, [M+H]⁺)/-4.7 ppm.

4.1.3.6. *N'-[(1E)-3-(4-nitrophenylhydrazono)]-(2E)-propan-2-ylidene-4-(N,N-dimethylamino)benzohydrazide (SintMed59)*. Yellow solid, yield 90%; mp 311.5–312.9 °C; R_f 0.52 (AcOEt); IR (KBr, ν_{max} cm⁻¹): 3394, 3190, 3134 (N-H), 3062, 3018 (C-H Ar), 2914, 2864 (C-H), 1651 (C=O), 1608 (C=C), 1569 (C=N); ¹H NMR (400 MHz, DMSO-*d*₆, δ ppm): 11.4 (s, 1H, NH), 10.4 (s, 1H, CONH), 8.16 (d, 2H, ³J = 8.8 Hz, 4-NO₂Ph H-3,5), 7.78 (d, 2H, ³J = 8.8 Hz, 4-NMe₂Ph H-2,6), 7.74 (s, 1H, N=CH), 7.16 (d, 2H, ³J = 9.2 Hz, 4-NO₂Ph H-2,6), 6.74 (d, 2H, ³J = 9.2 Hz, 4-NMe₂Ph H-3,5), 3.00 (s, 6H, NMe₂), 2.26 (s, 3H, CH₃); ¹³C NMR (100 MHz, DMSO-*d*₆, δ ppm): 152.4 (1C, 4-NMe₂Ph C-4), 150.8 (1C, CH₃C=N), 149.9 (1C, 4-NO₂Ph C-1), 142.5 (1C, N=CH), 138.8 (1C, 4-NO₂Ph C-4), 129.6 (2C, 4-NMe₂Ph C-2,6), 125.9 (2C, 4-NO₂Ph C-3,5), 119.5 (1C, 4-NMe₂Ph C-1), 111.5 (2C, 4-NO₂Ph C-2,6), 110.6 (2C, 4-NMe₂Ph C-3,5), 39.5 (2C, NMe₂), 10.9 (1C, CH₃); UHPLC-TOF-MS for C₁₈H₂₀N₆O₃ calcd (found)/Error: 367.1514 (367.1519, [M-H]⁻)/-1.4 ppm; 369.1696 (369.1675, [M+H]⁺)/5.7 ppm.

4.1.3.7. *N'-[(1E)-3-(4-nitrophenylhydrazono)]-(2E)-propan-2-ylidene-4-chlorobenzohydrazide (SintMed60)*. Yellow solid, yield 91%; mp 292.9–294.7 °C (dec); R_f 0.73 (AcOEt); IR (KBr, ν_{max} cm⁻¹): 3291, 3226 (N-H), 3062 (C-H Ar), 2970, 2924 (C-H), 1677 (C=O), 1635 (C=C), 1596 (C=N); ¹H NMR (400 MHz, DMSO-*d*₆, δ ppm): 11.5 (s, 1H, NH), 10.9 (s, 1H, CONH), 8.14 (d, 2H, ³J = 8.8 Hz, 4-NO₂Ph H-3,5), 7.88 (br d, 2H, ³J = 6.8 Hz, 4-ClPh H-2,6), 7.73 (s, 1H, N=CH), 7.56 (d, 2H, ³J = 8.4 Hz, 4-ClPh H-3,5), 7.16 (d, 2H, ³J = 8.8 Hz, 4-NO₂Ph H-2,6), 2.26 (s, 3H, CH₃); ¹³C NMR (100 MHz, DMSO-*d*₆, δ ppm): 163.0 (1C, C=O), 153.7 (1C, CH₃C=N), 149.8 (1C, 4-NO₂Ph C-1), 142.0 (1C, N=CH), 139.1 (1C, 4-NO₂Ph C-4), 136.3 (1C, 4-ClPh C-4), 132.3 (1C, 4-ClPh C-1), 130.0 (2C, 4-ClPh C-2,6), 128.2 (2C, 4-ClPh C-3,5), 126.0 (2C, 4-NO₂Ph C-3,5), 111.6 (2C, 4-NO₂Ph C-2,6), 11.3 (1C, CH₃); UHPLC-TOF-MS for C₁₆H₁₄N₅ClO₃ calcd (found)/Error: 358.0707 (358.0707, [M-H]⁻)/0.0 ppm; 360.0856 (360.0863, [M+H]⁺)/-1.9 ppm.

4.1.3.8. *N'-[(1E)-3-(4-nitrophenylhydrazono)]-(2E)-propan-2-ylidene-4-hydroxybenzohydrazide (SintMed61)*. Yellow solid, yield 92%; mp 307.5–308.6 °C (dec); R_f 0.37 (AcOEt); IR (KBr, ν_{max} cm⁻¹): 3386 (O-H), 3216, 3134 (N-H), 3060, 3022 (C-H Ar), 2916 2811 (C-H), 1654 (C=O), 1609 (C=C), 1594 (C=N); ¹H NMR (400

MHz, DMSO-*d*₆, δ ppm): 11.4 (s, 1H, NH), 10.5 (s, 1H, CONH), 10.1 (br s, 1H, OH), 8.15 (d, 2H, ³J = 8.8 Hz, 4-NO₂Ph H-3,5), 7.78 (d, 2H, ³J = 8.4 Hz, 4-OHPh H-2,6), 7.74 (s, 1H, N=CH), 7.16 (d, 2H, ³J = 8.8 Hz, 4-NO₂Ph H-2,6), 6.85 (d, 2H, ³J = 8.0 Hz, 4-OHPh H-3,5), 2.26 (s, 3H, CH₃); ¹³C NMR (100 MHz, DMSO-*d*₆, δ ppm): 160.6 (1C, C=O), 151.6 (2C, 4-OHPh C-4 and CH₃C=N), 149.9 (1C, 4-NO₂Ph C-1), 142.3 (1C, N=CH), 138.9 (1C, 4-NO₂Ph C-4), 130.2 (2C, 4-OHPh C-2,6), 125.9 (2C, 4-NO₂Ph C-3,5), 123.9 (1C, 4-OHPh C-1), 114.7 (2C, 4-OHPh C-3,5), 111.5 (2C, 4-NO₂Ph C-2,6), 11.0 (1C, CH₃); UHPLC-TOF-MS for C₁₆H₁₅N₅O₄ calcd (found)/Error: 340.1069 (340.1046, [M-H]⁻)/6.8 ppm; 342.1183 (342.120, [M+H]⁺)/-5.6 ppm.

4.1.3.9. *N'-[(1E)-3-(4-nitrophenylhydrazono)]-(2E)-propan-2-ylidene-4-nitrobenzohydrazide (SintMed62)*. Orange solid, yield 89%; mp 298.7–299.9 °C (dec); R_f 0.31 (AcOEt); IR (KBr, ν_{max} cm⁻¹): 3222, 3198 (N-H), 3077, 3061 (C-H Ar), 2968, 2913 (C-H), 1677 (C=O), 1595 (C=C), 1563 (C=N); ¹H NMR (400 MHz, DMSO-*d*₆, δ ppm): 11.5 and 11.3 (br s, 1H, NH), 11.3 and 11.1 (br s, 1H, CONH), 8.33 (d, 2H, ³J = 7.6 Hz, 4-NO₂Ph H-3,5), 8.15 (d, 2H, ³J = 8.8 Hz, 4-NO₂PhCONH H-2,6), 8.10 (br d, 2H, ³J = 8.8 Hz, 4-NO₂PhCONH H-3,5), 7.77 (s, 1H, N=CH), 7.17 (br d, 2H, ³J = 6.8 Hz, 4-NO₂Ph H-2,6), 2.28 (s, 3H, CH₃); ¹³C NMR (100 MHz, DMSO-*d*₆, δ ppm): 162.4 (1C, C=O), 154.5 (1C, CH₃C=N), 149.8 (1C, 4-NO₂PhCONH C-4), 149.1 (1C, 4-NO₂Ph C-1), 141.8 (1C, N=CH), 139.4 (1C, 4-NO₂Ph C-4), 139.1 (1C, 4-NO₂PhCONH C-1), 129.5 (2C, 4-NO₂PhCONH C-2,6), 126.0 (2C, 4-NO₂PhCO C-3,5), 123.3 (2C, 4-NO₂Ph C-3,5), 111.6 (2C, 4-NO₂Ph C-2,6), 11.5 (1C, CH₃); UHPLC-TOF-MS for C₁₆H₁₄N₆O₅ calcd (found)/Error: 369.0956 (369.0947, [M-H]⁻)/2.4 ppm; 371.1095 (371.110, [M+H]⁺)/-2.4 ppm.

4.1.3.10. *N'-[(1E)-3-(4-nitrophenylhydrazono)]-(2E)-propan-2-ylidene-3-methoxy-4-hydroxybenzohydrazide (SintMed63)*. Orange solid, yield 92%; mp 300.2–301.8 °C; R_f 0.48 (AcOEt); IR (KBr, ν_{max} cm⁻¹): 3486 (O-H), 3217, 3193 (N-H), 3063, 3024 (C-H Ar), 1655 (C=O), 1596 (C=C), 1568 (C=N); ¹H NMR (300 MHz, DMSO-*d*₆, δ ppm): 11.4 (s, 1H, NH), 10.6 (s, 1H, CONH), 9.71 (s, 1H, OH), 8.15 (d, 2H, ³J = 9.3 Hz, 4-NO₂Ph H-3,5), 7.75 (s, 1H, N=CH), 7.44 (s, 1H, Vaniliny H-2), 7.42 (d, 1H, ³J = 8.8 Hz, Vaniliny H-6), 7.16 (d, 2H, ³J = 9.3 Hz, 4-NO₂Ph H-2,6), 6.87 (d, 1H, ³J = 9.0 Hz, Vaniliny H-5), 3.84 (s, 3H, OCH₃), 2.27 (s, 3H, CH₃); ¹³C NMR (75 MHz, DMSO-*d*₆, δ ppm): 163.7 (1C, C=O), 152.0 (1C, CH₃C=N), 150.1 (1C, Vaniliny C-4), 149.9 (1C, 4-NO₂Ph C-1), 147.1 (1C, Vaniliny C-3), 142.3 (1C, N=CH), 138.9 (1C, 4-NO₂Ph C-4), 126.0 (2C, 4-NO₂Ph C-3,5), 124.2 (1C, Vaniliny C-1), 121.9 (1C, Vaniliny C-6), 114.7 (1C, Vaniliny C-5), 112.2 (1C, Vaniliny C-2), 111.5 (2C, 4-NO₂Ph C-2,6), 55.6 (1C, OCH₃), 11.1 (1C, CH₃); UHPLC-TOF-MS for C₁₇H₁₇N₅O₅ calcd (found)/Error: 370.1175 (370.1151, [M-H]⁻)/6.5 ppm; 372.1286 (372.1308, [M+H]⁺)/-5.9 ppm.

4.1.3.11. *N'-[(1E)-3-(4-nitrophenylhydrazono)]-(2E)-propan-2-ylidene-benzo[d][1,3]dioxole-5-carbohydrazide (SintMed64)*. Yellow solid, yield 78%; mp 305.2–306.0 °C; R_f 0.40 (AcOEt/Hexanes 7:3); IR (KBr, ν_{max} cm⁻¹): 3222, 3198, 3142 (N-H), 3064, 3024 (C-H Ar), 2971 (C-H), 1664 (C=O), 1643 (C=C), 1596 (C=N); ¹H NMR (400 MHz, DMSO-*d*₆, δ ppm): 11.4 (s, 1H, NH), 10.6 (s, 1H, CONH), 8.15 (d, 2H, ³J = 9.2 Hz, 4-NO₂Ph H-3,5), 7.73 (s, 1H, N=CH), 7.49 (dd, 1H, ³J = 8.0 Hz, ⁴J = 1.2 Hz, Piperonyl H-4), 7.43 (d, 1H, ⁴J = 1.6 Hz, Piperonyl H-6), 7.16 (d, 2H, ³J = 8.8 Hz, 4-NO₂Ph H-2,6), 7.03 (d, 1H, Piperonyl H-3), 6.12 (s, 2H, CH₂), 2.26 (s, 3H, CH₃); ¹³C NMR (100 MHz, DMSO-*d*₆, δ ppm): 163.6 (1C, C=O), 153.1 (1C, CH₃C=N), 150.6 (1C, Piperonyl C-2), 150.4 (1C, 4-NO₂Ph C-1), 147.6 (1C, Piperonyl C-1), 142.7 (1C, N=CH), 139.5 (1C, 4-NO₂Ph C-4), 127.8 (1C, Piperonyl C-5), 126.5 (2C, 4-NO₂Ph C-3,5), 123.9 (1C, Piperonyl C-6), 112.1 (2C, 4-NO₂Ph C-2,6), 108.7 (1C, Piperonyl C-4), 108.3 (1C, Piperonyl C-3), 102.2 (1C, CH₂), 11.7 (1C, CH₃);

UHPLC-TOF-MS for $C_{17}H_{15}N_5O_5$ calcd (found)/Error: 368.0998 (368.0995, $[M-H]^-$)/0.8 ppm; 370.1150 (370.1151, $[M+H]^+$)/-0.3 ppm.

4.1.3.12. *N'-[(1E)-3-(4-nitrophenylhydrazono)]-(2E)-propan-2-ylidene-3,5-dinitrobenzohydrazide (SintMed65)*. Yellow solid, yield 92%; mp 276.2–276.9 °C; R_f 0.30 (AcOEt); IR (KBr, ν_{max} cm^{-1}): 3253, 3196, 3103 (N–H), 2876 (C–H), 1661 (s, C=O), 1604 (C=C), 1595 (C=N); 1H NMR (400 MHz, DMSO- d_6 , δ ppm): 11.6 e 11.45 (br s, 1H, NH), 11.45 e 11.39 (s, 1H, CONH), 9.03–8.96 (br m, 3H, 3,5-diNO₂Ph H-2,4), 8.17 (d, 2H, $^3J = 8.8$ Hz, 4-NO₂Ph H-3,5), 7.78 (s, 1H, N=CH), 7.20 (br d, 2H, $^3J = 8.4$ Hz, 4-NO₂Ph H-2,6), 2.33 e 2.25 (s, 3H, CH₃); ^{13}C NMR (100 MHz, DMSO- d_6 , δ ppm): 160.2 (1C, C=O), 155.3 (1C, CH₃C=N), 149.7 (1C, 4-NO₂Ph C-1), 147.8 (2C, 3,5-diNO₂Ph C-3,5), 141.5 (1C, N=CH), 139.2 (1C, 4-NO₂Ph C-4), 129.8 (1C, 3,5-diNO₂Ph C-1), 128.4 (2C, 3,5-diNO₂Ph C-2,6), 121.0 (1C, 3,5-diNO₂Ph C-4), 111.7 (2C, 4-NO₂Ph C-2,6), 11.9 (1C, CH₃); Anal Calcd for $C_{16}H_{13}N_7O_7$: C, 46.26; H, 3.16; N, 23.61; Found: C, 46.28; H, 3.12; N, 23.65.

4.1.3.13. *N'-[(1E)-3-(4-nitrophenylhydrazono)]-(2E)-propan-2-ylidene-2-methylbenzohydrazide (SintMed66)*. Yellow solid, yield 81%; mp 252.5–253.4 °C; R_f 0.47 (AcOEt/Hexanes 7:3); IR (KBr, ν_{max} cm^{-1}): 3293, 3239, 3203 (N–H), 3091 (C–H Ar), 1669 (C=O), 1592 (C=C), 1567 (C=N); 1H NMR (400 MHz, DMSO- d_6 , δ ppm): 11.5 and 11.2 (s, 1H, NH), 11.2 and 10.9 (s, 1H, CONH), 8.15 (d, 2H, $^3J = 8.0$ Hz, 4-NO₂Ph H-3,5), 7.76 (s, 1H, N=CH), 7.45–7.07 (m, 4H, 2-CH₃Ph H-3,4,5,6), 7.16 (d, 2H, $^3J = 8.0$ Hz, 4-NO₂Ph H-2,6), 2.37 (s, 3H, 2-CH₃Ph), 2.23 and 2.19 (s, 3H, CH₃); ^{13}C NMR (100 MHz, DMSO- d_6 , δ ppm): 165.6 (1C, C=O), 152.4 (1C, CH₃C=N), 149.9 (1C, 4-NO₂Ph C-1), 142.2 (1C, N=CH), 139.0 (1C, 4-NO₂Ph C-4), 135.8, 135.4, 130.4, 129.8, 127.8 (5C, 2-CH₃Ph), 126.1 and 125.4 (2C, 4-NO₂Ph C-3,5), 111.6 (3C, 4-NO₂Ph C-3,5 and 2-CH₃Ph), 19.3 (1C, 2-CH₃Ph), 11.4 (1C, CH₃); UHPLC-TOF-MS for $C_{17}H_{17}N_5O_3$ calcd (found)/Error: 338.1259 (338.1253, $[M-H]^-$)/1.8 ppm; 340.1407 (340.1410, $[M+H]^+$)/-0.9 ppm.

4.1.3.14. *N'-[(1E)-3-(4-nitrophenylhydrazono)]-(2E)-propan-2-ylidene-3-methylbenzohydrazide (SintMed67)*. Yellow solid, yield 74%; mp 302.0–303.2 °C; R_f 0.41 (AcOEt/Hexanes 7:3); IR (KBr, ν_{max} cm^{-1}): 3367, 3271, 3197 (N–H), 3061, 3027 (C–H Ar), 2923 (C–H), 1650 (C=O), 1597 (C=C), 1567 (C=N); 1H NMR (300 MHz, DMSO- d_6 , δ ppm): 11.5 (s, 1H, NH), 10.8 (s, 1H, CONH), 8.16 (d, 2H, $^3J = 9.3$ Hz, 4-NO₂Ph H-3,5), 7.74 (s, 1H, N=CH), 7.67 (br s, 2H, 3-CH₃Ph H-2,6), 7.40 (br s, 2H, 3-CH₃Ph H-4,5), 7.17 (d, 2H, $^3J = 9.3$ Hz, 4-NO₂Ph H-2,6), 2.39 (s, 3H, 3-CH₃Ph), 2.27 (s, 3H, CH₃); ^{13}C NMR (75 MHz, DMSO- d_6 , δ ppm): 149.9 (1C, 4-NO₂Ph C-1), 142.2 (1C, N=CH), 139.0 (1C, 4-NO₂Ph C-4), 137.5 (1C, 3-CH₃Ph C-3), 133.6 (1C, 3-CH₃Ph C-1), 132.1 (1C, 3-CH₃Ph C-4 or C-5), 128.4 (1C, 3-CH₃Ph C-2 or C-6), 128.1 (1C, 3-CH₃Ph C-4 or C-5), 126.0 (2C, 4-NO₂Ph C-3,5), 125.2 (1C, 3-CH₃Ph C-2 or C-6), 111.6 (2C, 4-NO₂Ph C-2,6), 28.5 (1C, 3-CH₃Ph), 11.2 (1C, CH₃); UHPLC-TOF-MS for $C_{17}H_{17}N_5O_3$ calcd (found)/Error: 338.1265 (338.1253, $[M-H]^-$)/3.5 ppm; 340.1414 (340.1410, $[M+H]^+$)/1.2 ppm.

4.1.3.15. *N'-[(1E)-3-(4-nitrophenylhydrazono)]-(2E)-propan-2-ylidene-2-fluorobenzohydrazide (SintMed68)*. Yellow solid, yield 93%; mp 298.8–300.2 °C (dec); R_f 0.68 (AcOEt); IR (KBr, ν_{max} cm^{-1}): 3405, 3230, 3206, 3150 (N–H), 3090, 3072 (C–H Ar), 2925 (C–H), 1664 (C=O), 1599 (C=C), 1568 (C=N); 1H NMR (400 MHz, DMSO- d_6 , δ ppm): 11.3 (br s, 2H, NH and CONH), 8.15 (d, 2H, $^3J = 8.4$ Hz, 4-NO₂Ph H-3,5), 7.76 (s, 1H, N=CH), 7.71–7.08 (m, 4H, 2-FPh H-3,4,5,6), 7.17 (d, 2H, $^3J = 8.0$ Hz, 4-NO₂Ph H-2,6), 2.21 and 2.17 (s, 3H, CH₃); ^{13}C NMR (100 MHz, DMSO- d_6 , δ ppm): 160.6 (1C, C=O), 158.0 (1C, Ar), 152.7 (1C, CH₃C=N), 149.8 (1C, 4-NO₂Ph C-1), 142.1 and 141.8 (1C, N=CH), 139.0 (1C, 4-NO₂Ph

C-4), 132.8, 132.7, 131.6, 130.3, 129.4 (2C, Ar), 126.0 (2C, 4-NO₂Ph C-3,5), 124.4, 124.0, 123.0, 122.9, 116.1, 115.9 (2C, Ar), 111.6 (2C, 4-NO₂Ph C-2,6), 11.2 and 10.9 (1C, CH₃); ^{19}F NMR (376 MHz, DMSO- d_6 , δ ppm): -113.0 and -113.3 (s, 1F, 2-FPh); UHPLC-TOF-MS for $C_{16}H_{14}N_5FO_3$ calcd (found)/Error: 342.0994 (342.1002, $[M-H]^-$)/-2.3 ppm; 344.1176 (344.1159, $[M+H]^+$)/4.9 ppm.

4.1.3.16. *N'-[(1E)-3-(4-nitrophenylhydrazono)]-(2E)-propan-2-ylidene-2-chlorobenzohydrazide (SintMed69)*. Yellow solid, yield 89%; mp 287.3–288.0 °C; R_f 0.63 (AcOEt/Hexanes 7:3); IR (KBr, ν_{max} cm^{-1}): 3300, 3241, 3205 (N–H), 3092 (C–H Ar), 1671 (C=O), 1592 (C=C), 1568 (C=N); 1H NMR (300 MHz, DMSO- d_6 , δ ppm): 11.5 and 11.4 (s, 1H, NH), 11.2 and 11.1 (s, 1H, CONH), 8.14 (d, 2H, $^3J = 9.3$ and 11.7 Hz, 4-NO₂Ph H-3,5), 7.76 (s, 1H, N=CH), 7.57–7.36 (m, 4H, 2-ClPh H-3,4,5,6), 7.16 and 7.06 (d, 2H, $^3J = 8.7$ and 9.0 Hz, 4-NO₂Ph H-2,6), 2.18 and 2.16 (s, 3H, CH₃); ^{13}C NMR (75 MHz, DMSO- d_6 , δ ppm): 169.3 (1C, 2-ClPh C-1), 162.9 (1C, C=O), 152.9 (1C, CH₃C=N), 149.8 and 149.7 (1C, 4-NO₂Ph C-1), 148.4 (1C, 2-ClPh C-2), 142.2 and 141.9 (1C, N=CH), 139.0 and 138.9 (1C, 4-NO₂Ph C-4), 136.1, 135.2, 135.4, 131.1, 130.4, 130.3, 129.5, 128.8, 128.5, 127.0 and 126.7 (4C, 2-ClPh C-3,4,5,6), 126.0 (2C, 4-NO₂Ph C-3,5), 111.6 and 111.4 (2C, 4-NO₂Ph C-2,6), 11.5 and 10.9 (1C, CH₃); UHPLC-TOF-MS for $C_{16}H_{14}N_5ClO_3$ calcd (found)/Error: 358.0721 (358.0707, $[M-H]^-$)/3.9 ppm; 360.0883 (360.0863, $[M+H]^+$)/5.6 ppm.

4.1.3.17. *N'-[(1E)-3-(4-nitrophenylhydrazono)]-(2E)-propan-2-ylidene-2-iodobenzohydrazide (SintMed70)*. Yellow solid, yield 79%; mp 251.5–252.7 °C; R_f 0.63 (AcOEt/Hexanes 7:3); IR (KBr, ν_{max} cm^{-1}): 3227, 3239, 3202 (N–H), 3075, 3025 (C–H Ar), 1678 (C=O), 1596 (C=C), 1566 (C=N); 1H NMR (400 MHz, DMSO- d_6 , δ ppm): 11.5 and 11.4 (s, 1H, NH), 11.2 and 11.1 (s, 1H, CONH), 8.17–8.10 (m, 2H, 4-NO₂Ph H-3,5), 7.92 and 7.85 (d, 1H, $^3J = 8.0$ Hz, Ar), 7.76 (s, 1H, N=CH), 7.51–7.05 (m, 6H, Ar), 2.20 and 2.16 (s, 3H, CH₃); ^{13}C NMR (100 MHz, DMSO- d_6 , δ ppm): 171.3 and 165.4 (1C, C=O), 152.9 (1C, CH₃C=N), 149.9 and 148.2 (1C, 4-NO₂Ph C-1), 142.3 and 142.2 (1C, N=CH), 141.9, 141.3, 139.0, 138.9, 138.1 (3C, Ar), 131.1, 130.1, 128.7, 128.0, 127.8, 127.5 (3C, Ar), 126.0 (2C, 4-NO₂Ph C-3,5), 111.6 and 111.4 (2C, Ar), 94.1 and 93.4 (1C, Ar), 11.5 and 10.9 (1C, CH₃); UHPLC-TOF-MS for $C_{16}H_{14}N_5IO_3$ calcd (found)/Error: 450.0060 (450.0063, $[M-H]^-$)/-0.7 ppm; 452.0210 (452.0220, $[M+H]^+$)/-2.2 ppm.

4.1.3.18. *N'-[(1E)-3-(4-nitrophenylhydrazono)]-(2E)-propan-2-ylidene-2-hydroxybenzohydrazide (SintMed71)*. Yellow solid, yield 93%; mp 305.7–306.5 °C (dec); R_f 0.45 (AcOEt); IR (KBr, ν_{max} cm^{-1}): 3308–2935 (O–H), 3308, 3243, 3211, 3160 (N–H), 3079 (C–H Ar), 2935 (C–H), 1646 (s, C=O), 1599 (C=C), 1555 (C=N); 1H NMR (400 MHz, DMSO- d_6 , δ ppm): 11.8 (br s, 1H, OH), 11.5 (s, 1H, NH), 11.4 (s, 1H, CONH), 8.15 (d, 2H, $^3J = 8.4$ Hz, 4-NO₂Ph H-3,5), 7.98 (d, 1H, $^3J = 7.6$ Hz, 2-OHPh H-6), 7.78 (s, 1H, N=CH), 7.42 (t, 1H, $^3J = 7.2$ Hz, 2-OHPh H-4), 7.17 (d, 2H, $^3J = 8.0$ Hz, 4-NO₂Ph H-2,6), 7.04–6.96 (m, 2H, 2-OHPh H-3,5), 2.22 (s, 3H, CH₃); ^{13}C NMR (100 MHz, DMSO- d_6 , δ ppm): 161.4 (1C, C=O), 156.1 (1C, 2-OHPh C-2), 151.0 (1C, CH₃C=N), 149.9 (1C, 4-NO₂Ph C-1), 141.8 (1C, N=CH), 139.0 (1C, 4-NO₂Ph C-4), 133.5 (1C, 2-OHPh C-4), 130.8 (1C, 2-OHPh C-6), 126.0 (2C, 4-NO₂Ph C-3,5), 119.7 (1C, 2-OHPh C-3 or C-5), 117.7 (1C, 2-OHPh C-1), 116.8 (1C, 2-OHPh C-3 or C-5), 111.6 (2C, 4-NO₂Ph C-2,6), 10.6 (1C, CH₃); UHPLC-TOF-MS for $C_{16}H_{15}N_5O_4$ calcd (found)/Error: 340.1044 (340.1046, $[M-H]^-$)/-0.6 ppm; 342.1165 (342.1202, $[M+H]^+$)/-3.7 ppm.

4.1.3.19. *N'-[(1E)-3-(4-nitrophenylhydrazono)]-(2E)-propan-2-ylidene-2-phenoxybenzohydrazide (SintMed72)*. Yellow solid, yield 91%; mp 263.1–264.6 °C; R_f 0.39 (AcOEt/Hexanes 7:3); IR (KBr, ν_{max} cm^{-1}): 3351, 3226, 3199 (N–H), 3067 (C–H Ar), 1667 (C=O), 1593

(C=C), 1528 (C=N); ^1H NMR (400 MHz, DMSO- d_6 , δ ppm): 11.48 and 11.21 (s, 1H, NH), 11.16 and 10.95 (s, 1H, CONH), 8.13 (d, 2H, $^3J = 8.8$ Hz, 4-NO $_2$ Ph H-3,5), 7.83 (d, 1H, $^3J = 6.4$ Hz, Ar), 7.72 (s, 1H, N=CH), 7.54–6.91 (m, 10H, Ar), 2.12 and 2.07 (s, 3H, CH $_3$); ^{13}C NMR (100 MHz, DMSO- d_6 , δ ppm): 161.5 (1C, C=O), 155.7 (1C, Ar), 154.2 (1C, Ar), 151.7 (1C, CH $_3$ C=N), 149.8 (1C, 4-NO $_2$ Ph C-1), 141.8 (1C, N=CH), 139.0 (1C, 4-NO $_2$ Ph C-4), 132.5, 130.6, 129.6 (6C, Ar), 126.0 and 125.5 (2C, 4-NO $_2$ Ph C-3,5), 124.1, 123.5, 118.9, 118.3, 111.6 and 111.4 (6C, Ar), 10.7 (1C, CH $_3$); Anal Calcd for C $_{22}$ H $_{19}$ N $_5$ O $_4$: C, 63.29; H, 4.60; N, 16.78; Found: C, 63.25; H, 4.57; N, 16.80.

4.1.3.20. *N'-[(1E)-3-(4-nitrophenylhydrazono)]-(2E)-propan-2-ylidene-2-aminobenzohydrazide (SintMed73)*. Yellow solid, yield 91%; mp 272.0–274.3 °C (dec); R $_f$ 0.50 (AcOEt); IR (KBr, ν_{max} cm $^{-1}$): 3431, 3409, 3325, 3227 (N–H), 3072 (C–H Ar), 1644 (C=O), 1598 (C=C), 1568 (C=N); ^1H NMR (400 MHz, DMSO- d_6 , δ ppm): 11.5 (s, 1H, NH), 10.6 (s, 1H, CONH), 8.15 (d, 2H, $^3J = 8.8$ Hz, 4-NO $_2$ Ph H-3,5), 7.74 (s, 1H, N=CH), 7.54 (d, 1H, $^3J = 7.6$ Hz, 2-NH $_2$ Ph H-6), 7.21 (t, 1H, $^3J = 7.6$ Hz and 8.0 Hz, 2-NH $_2$ Ph H-4), 7.16 (d, 2H, $^3J = 8.8$ Hz, 2-NO $_2$ Ph H-2,6), 6.77 (d, 1H, $^3J = 8.0$ Hz, 2-NH $_2$ Ph H-3), 6.58 (t, 1H, $^3J = 7.2$ and 7.6 Hz, 2-NH $_2$ Ph H-5), 6.22 (br s, 2H, NH $_2$), 2.25 (s, 3H, CH $_3$); ^{13}C NMR (100 MHz, DMSO- d_6 , δ ppm): 165.8 (1C, C=O), 151.8 (1C, CH $_3$ C=N), 149.9 (1C, 4-NO $_2$ Ph C-1), 149.6 (1C, 2-NH $_2$ Ph C-2), 142.3 (1C, N=CH), 138.9 (1C, 4-NO $_2$ Ph C-4), 132.2 (1C, 2-NH $_2$ Ph C-4), 129.1 (1C, 2-NH $_2$ Ph C-6), 126.0 (2C, 4-NO $_2$ Ph C-3,5), 116.2 (1C, 2-NH $_2$ Ph C-3), 114.7 (1C, 2-NH $_2$ Ph C-5), 114.1 (1C, 2-NH $_2$ Ph C-1), 111.5 (2C, 4-NO $_2$ Ph C-2,6), 11.1 (1C, CH $_3$); UHPLC-TOF-MS for C $_{16}$ H $_{16}$ N $_6$ O $_3$ calcd (found)/Error: 339.1216 (339.1206, [M–H] $^-$)/2.9 ppm; 341.1337 (341.1362, [M+H] $^+$)/–7.3 ppm.

4.1.3.21. *N'-[(1E)-3-(4-nitrophenylhydrazono)]-(2E)-propan-2-ylidene-2-(N-phenylamino)benzohydrazide (SintMed74)*. Yellow solid, yield 93%; mp 254.1–256.0 °C; R $_f$ 0.46 (AcOEt/Hexanes 1:1); IR (KBr, ν_{max} cm $^{-1}$): 3245, 3224, 3205 (N–H), 3048, 3021 (C–H Ar), 1640 (C=O), 1595 (C=C), 1570 (C=N); ^1H NMR (400 MHz, DMSO- d_6 , δ ppm): 11.5 (s, 1H, NH), 11.0 (s, 1H, CONH), 8.02 (br s, 1H, NHPh), 8.14 (d, 2H, $^3J = 9.2$ Hz, 4-NO $_2$ Ph H-3,5), 7.72 (br s, 2H, N=CH and Ar), 7.41 (t, 1H, $^3J = 8.4$ Hz, Ar), 7.32–7.25 (m, 3H, Ar), 7.15 (d, 2H, $^3J = 9.2$ Hz, 4-NO $_2$ Ph H-2,6), 7.09 (d, 2H, $^3J = 7.6$ Hz, Ar), 6.99–6.91 (m, 2H, Ar), 2.20 (s, 3H, CH $_3$); ^{13}C NMR (100 MHz, DMSO- d_6 , δ ppm): 165.2 (1C, C=O), 152.4 (1C, CH $_3$ C=N), 149.8 (1C, 4-NO $_2$ Ph C-1), 143.3 (1C, Ar), 142.2 (1C, N=CH), 142.0 (1C, Ar), 139.0 (1C, 4-NO $_2$ Ph C-4), 132.1, 130.0, 129.2 (6C, Ar), 126.0 (2C, 4-NO $_2$ Ph C-3,5), 121.2, 119.5, 118.4, 117.3 (), 111.6 (2C, 4-NO $_2$ Ph C-2,6), 11.0 (1C, CH $_3$); Anal Calcd for C $_{22}$ H $_{20}$ N $_6$ O $_3$: C, 63.44; H, 4.85; N, 20.18; Found: C, 63.46; H, 4.83; N, 20.20.

4.1.4. Synthesis of α -oxopropane-4-nitrophenyl-N-methylhydrazone (6)

In a round bottom flask, compound **5** (0.5000 g, 2.41 mmol), potassium carbonate (1.0005 g, 7.24 mmol), methyl iodide (0.45 mL, 7.24 mmol) and 10.0 mL of acetone were mixed together, giving an intense red suspension, which was stirred at room temperature for 12 h. After this time, the suspension had turned yellow. The solvent was removed at room temperature under vacuum, the solid was suspended in 15 mL of water and heated at 65 °C for 10 min. After reached room temperature, the mixture was cooled, filtered off and the yellow solid washed with cold water. Compound **6** was used without further purification. Yield 95%; mp 184.1–185.1 °C; R $_f$ 0.41 (AcOEt/Hexanes 1:1); IR (KBr, ν_{max} cm $^{-1}$): 30116, 3066 (Ar C–H), 2925 (C–H), 1694, 1667 (C=C), 1594 (C=N); ^1H NMR (400 MHz, DMSO- d_6 , δ ppm): 8.22 (d, 2H, $^3J = 8.8$ Hz, 4-NO $_2$ Ph H-3,5), 7.66 (d, 2H, $^3J = 8.8$ Hz, 4-NO $_2$ Ph H-2,6), 7.23 (s, 1H, N=CH), 3.49 (s, 3H, NCH $_3$), 2.40 (s, 3H, CH $_3$); ^{13}C

NMR (100 MHz, DMSO- d_6 , δ ppm): 196.7 (1C, C=O), 150.9 (1C, 4-NO $_2$ Ph C-1), 141.5 (1C, 4-NO $_2$ Ph C-4), 134.9 (1C, N=CH), 125.2 (2C, 4-NO $_2$ Ph C-3,5), 115.6 (2C, 4-NO $_2$ Ph C-2,6), 33.5 (1C, NCH $_3$), 24.8 (1C, CH $_3$).

4.1.5. General procedure for the synthesis of N-methylated hydrazone-N-acylhydrazones SintMed(75–77)

To a stirred suspension of compound **6** (0.50 mmol) and the appropriate hydrazide (0.50 mmol) in 4.0 mL of ethanol, cerium (III) chloride heptahydrate (10 mol%) was added and the reaction mixture was stirred at 65 °C during 1–2 h. Reaction's completion was monitored by TLC, using appropriate eluent system. The reactional medium was allowed to reach room temperature, giving orange precipitates. After cooling, the solids were filtered off, and washed with cold ethanol. Recrystallization from ethanol afforded the samples for biological purposes, which were dried in an Abderhalden's apparatus to remove traces of solvent.

4.1.5.1. *N'-[(1E)-3-(N-methyl-4-nitrophenylhydrazono)]-(2E)-propan-2-ylidene-4-aminobenzohydrazide (SintMed75)*. Orange solid, yield 82%; mp 284.2–286.4 °C; R $_f$ 0.27 (AcOEt); IR (KBr, ν_{max} cm $^{-1}$): 3466, 3342, 3226 (N–H), 3022 (C–H Ar), 1642 (C=O), 1601 (C=C), 1574 (C=N); ^1H NMR (400 MHz, DMSO- d_6 , δ ppm): 10.3 (s, 1H, CONH), 8.17 (d, 2H, $^3J = 9.6$ Hz, 4-NO $_2$ Ph H-3,5), 7.66 (d, 2H, $^3J = 8.8$ Hz, 4-NH $_2$ Ph H-2,6), 7.63 (s, 1H, N=CH), 7.55 (d, 2H, $^3J = 9.2$ Hz, 4-NO $_2$ Ph H-2,6), 6.60 (d, 2H, $^3J = 8.8$ Hz, 4-NH $_2$ Ph H-3,5), 5.79 (s, 2H, NH $_2$), 3.51 (s, 3H, NCH $_3$), 2.30 (s, 3H, CH $_3$); ^{13}C NMR (100 MHz, DMSO- d_6 , δ ppm): 163.7 (1C, C=O), 152.3 (1C, CH $_3$ C=N), 151.6 (1C, 4-NH $_2$ Ph C-4), 151.3 (1C, 4-NO $_2$ Ph C-1), 139.5 (1C, 4-NO $_2$ Ph C-4), 138.6 (1C, N=CH), 129.8 (2C, 4-NH $_2$ Ph C-2,6), 125.3 (2C, 4-NO $_2$ Ph C-3,5), 119.5 (1C, 4-NH $_2$ Ph C-1), 113.4 (2C, 4-NO $_2$ Ph C-2,6), 112.4 (2C, 4-NH $_2$ Ph C-3,5), 32.7 (1C, NCH $_3$), 11.2 (1C, CH $_3$); UHPLC-TOF-MS for C $_{17}$ H $_{18}$ N $_6$ O $_3$ calcd (found)/Error: 353.1363 (353.1362, [M–H] $^-$)/0.3 ppm; 355.1514 (355.1519, [M+H] $^+$)/–1.4 ppm.

4.1.5.2. *N'-[(1E)-3-(N-methyl-4-nitrophenylhydrazono)]-(2E)-propan-2-ylidene-3,5-dinitrobenzohydrazide (SintMed76)*. Orange solid, yield 94%; mp 271.2–273.1 °C; R $_f$ 0.49 (AcOEt/MeOH 9.5:0.5); IR (KBr, ν_{max} cm $^{-1}$): 3371 (N–H), 3086 (C–H Ar), 2889 (C–H), 1697 (C=O), 1593 (C=C), 1545 (C=N); ^1H NMR (400 MHz, DMSO- d_6 , δ ppm): 11.4 (br s, 1H, CONH), 9.06 (s, 2H, 3,5-diNO $_2$ Ph H-2,6), 9.01 (s, 1H, 3,5-diNO $_2$ Ph H-4), 8.17 (d, 2H, $^3J = 9.4$ Hz, 4-NO $_2$ Ph H-3,5), 7.70 and 7.67 (br s, 1H, N=CH), 7.57 (br d, 2H, $^3J = 8.4$ Hz, 4-NO $_2$ Ph H-2,6), 3.54 e 3.50 (s, 3H, NCH $_3$), 2.40 and 2.37 (s, 3H, CH $_3$); ^{13}C NMR (100 MHz, DMSO- d_6 , δ ppm): 152.0 (1C, 4-NO $_2$ Ph C-1), 148.3 (2C, 3,5-diNO $_2$ Ph C-3,5), 140.6 (1C, N=CH), 128.9 (2C, 3,5-diNO $_2$ Ph C-2,6), 125.8 (2C, 4-NO $_2$ Ph C-3,5), 121.5 (1C, 3,5-diNO $_2$ Ph C-4), 114.7 (2C, 4-NO $_2$ Ph C-2,6), 33.5 (1C, NCH $_3$); UHPLC-TOF-MS for C $_{17}$ H $_{15}$ N $_7$ O $_7$ calcd (found)/Error: 428.0958 (428.0955, [M–H] $^-$)/0.7 ppm; 430.1101 (430.1111, [M+H] $^+$)/–2.3 ppm.

4.1.5.3. *N'-[(1E)-3-(N-methyl-4-nitrophenylhydrazono)]-(2E)-propan-2-ylidene-2-hydroxybenzohydrazide (SintMed77)*. Orange solid, yield 91%; mp 299.0–300.0 °C; R $_f$ 0.20 (AcOEt/MeOH 9.5:0.5); IR (KBr, ν_{max} cm $^{-1}$): 3422–2833 (O–H), 3263 (N–H), 3075, 3037 (C–H Ar), 2920 (C–H), 1644 (C=O), 1596 (C=C), 1563 (C=N); ^1H NMR (400 MHz, DMSO- d_6 , δ ppm): 11.6 (br s, 2H, OH and CONH), 8.25 and 8.18 (d, 2H, $^3J = 9.2$ Hz, 4-NO $_2$ Ph H-3,5), 8.00 (br s, 1H, 2-OHPh H-6), 7.70 and 7.68 (s, 1H, N=CH), 7.57 (d, 2H, $^3J = 9.6$ Hz, 4-NO $_2$ Ph H-2,6), 7.43 (t, 1H, $^3J = 7.2$ Hz, 2-OHPh H-4), 7.04–6.96 (m, 2H, 2-OHPh H-3,5), 3.54 and 3.50 (s, 3H, NCH $_3$), 2.40 and 2.28 (s, 3H, CH $_3$); ^{13}C NMR (100 MHz, DMSO- d_6 , δ ppm): 156.6 (1C, 2-OHPh C-2), 151.5 (1C, CH $_3$ C=N), 139.8 (1C, 4-NO $_2$ Ph C-1), 138.0 (1C, N=CH), 134.8 (1C, 4-NO $_2$ Ph C-4), 133.8

(1C, 2-OHPh C-4), 130.6 (1C, 2-OHPh C-6), 125.3 and 125.2 (2C, 4-NO₂Ph C-3,5), 119.5 (1C, 2-OHPh C-3 or C-5), 116.9 (1C, 2-OHPh C-3 or C-5), 115.6 (1C, 2-OHPh C-1), 113.9 (2C, 4-NO₂Ph C-2,6), 32.9 (1C, NCH₃), 11.0 (1C, CH₃); UHPLC-TOF-MS for C₁₇H₁₇N₅O₄ calcd (found)/Error: 354.1204 (354.1202, [M-H]⁻)/0.6 ppm; 356.1337 (356.1359, [M+H]⁺)/-6.2 ppm.

4.2. X-ray crystallographic analysis

The data collection was performed using Mo-Kα radiation ($\lambda = 0.71073 \text{ \AA}$) at 298 K on a BRUKER APEX II Duo diffractometer. Reduction and absorption correction were carried out with the Bruker SAINT package. The structure was solved with SHELXS97 using direct methods in OLEX2^[34,35] where all non-hydrogen atoms were refined with anisotropic displacement parameters with SHELXL97.³⁶ Hydrogen atoms were calculated at idealized positions using the riding model option of SHELXL97.³⁶ Orange crystals were obtained by slow evaporation in dichloromethane/tetrahydrofuran. Compound has crystallized in a monoclinic system and C2/c space group with four molecules for asymmetric unit. The molecular structure of the compounds is shown as an ORTEP representation in Fig. 2. The crystallographic data were deposited at CCDC (number 1554110).

4.3. Animals

BALB/c mice (4–10 weeks old) were bred and maintained at the Gonçalo Moniz Institute (Oswaldo Cruz Foundation, Bahia, Brazil), under a controlled environment and receiving a balanced rodent diet and water *ad libitum*. All animal experiments and procedures were approved by the institution's committee on the ethical handling of laboratory animals (Approval number: 018/2015).

4.4. Cytotoxicity to mammalian cells

Cytotoxicity of the compounds was determined using the murine macrophage cell line J774. Cells were seeded into 96-well plates at 1×10^4 cells/well in Dulbecco's modified Eagle medium (DMEM; Life Technologies, GIBCO-BRL, Gaithersburg, MD, USA) supplemented with 10% fetal bovine serum (FBS; GIBCO) and 50 $\mu\text{g/mL}$ of gentamycin (Life Technologies) and incubated for 24 h at 37 °C and 5% CO₂. The compounds test were then added (100–0.41 μM), in triplicate and incubated for 72 h. Gentian violet was used as positive control. Twenty μL /well of AlamarBlue (Invitrogen, Carlsbad, CA, USA) were added to the plates during 4 h. Colorimetric readings were performed at 570 and 600 nm. CC₅₀ values were calculated using data-points obtained from three independent experiments.

4.5. Assessment of nitric oxide production

J774 cells or peritoneal macrophages from BALB/c mice were seeded in 96-well tissue culture plates at 2×10^5 cells/well in DMEM medium supplemented with 10% of FBS and 50 $\mu\text{g/mL}$ of gentamycin for 2 h at 37 °C and 5% CO₂. Cells were then stimulated with LPS (from *Escherichia coli* O111:B4, 500 ng/mL, Sigma-Aldrich) and IFN γ (5 ng/mL; Sigma-Aldrich) in the absence or presence of compounds at different concentrations and incubated at 37 °C. Nitric oxide production was estimated in macrophage cultures harvested at 24 h by using the Griess method for nitrite quantification.³⁷ Percentage of nitric oxide inhibition was determined in comparison to stimulated and untreated control.

4.6. Inhibition of lymphoproliferation assay

BALB/c splenocyte suspensions were prepared in DMEM medium supplemented with 10% of FBS and 50 $\mu\text{g/mL}$ of gentamicin. Splenocytes (1×10^6 cells/well) were plated in 96-well plates, in triplicate, and stimulated or not with concanavalin A (Con A; 2 $\mu\text{g/mL}$, Sigma-Aldrich) or Dynabeads[®] mouse T-activator CD3/CD28 (bead to cell ratio = 1:1; ThermoFisher Scientific, Waltham, MA, USA). Splenocytes were activated in the absence or presence of various concentrations of compounds (12–0.04 μM). After 48 h of incubation, 1 μCi of ³H–thymidine was added to each well, and plates were incubated for additional 18 h. Plates were read using a scintillation counter Chameleon (Hydex; Turku, Finland). Cell proliferation was measured as the percent of ³H-thymidine incorporation for treated-cells in comparison to untreated cells. Dexamethasone was used as positive control. IC₅₀ values were calculated using data from three independent experiments.

4.7. Assessment of cytokines, PGE2 and COX2

for quantification of cytokine production by macrophages, cell-free supernatants from BALB/c peritoneal macrophage cultures were collected 4 h (for TNF α and IL-6) and 24 h (for IL-1 β) after challenge with LPS + IFN γ . For quantification of IL-2, IL-4, IL-10, IL-17 and IFN γ in splenocyte cultures, cells were plated into 24-well plates at 5×10^6 cells/well in DMEM containing or not 5 $\mu\text{g/mL}$ of Con A in the absence or presence of different concentrations of **SintMed65** (10, 5 and 2.5 μM). After 48 h of culture, cell free supernatants were harvested and stored at -80 °C for cytokine analysis. The concentration of cytokines in culture supernatants was determined by enzyme-linked immunosorbent assay (ELISA) using DuoSet kits from R&D Systems (Minneapolis, MN) according to the manufacturer's instructions. PGE2 was determined in the supernatant of J774 cells by enzyme immunoassay (EIA) using DRG Prostaglandin E2 kit (DRG Instruments, Marburg, Germany). Gene expression of cyclooxygenase 2 (COX2) was assessed by quantitative real-time reverse transcription polymerase chain reaction (qRT-PCR) by extracting RNA of J774 cells using TRIzol reagent (Invitrogen, Molecules Probes, Eugene, OR). Then, cDNA was synthesized from 1 μg of RNA using High Capacity cDNA Reverse Transcription kit (Applied Biosystems, Foster City, CA, USA). The qRT-PCR amplification mixtures contained template cDNA, TaqMan Master Mix and probes (all from Applied Biosystems). All reactions were run in triplicate on an ABI7500 Sequence Detection System (Applied Biosystems) under standard thermal cycling conditions. A non template control (NTC) and non-reverse transcription controls (No-RT) were also included. The samples were normalized with 18S and *Hprt*. The threshold cycle ($2^{-\Delta\Delta\text{Ct}}$) method of comparative PCR was used to analyze the results.³⁸

4.8. Cell cycle analysis

Splenocytes from BALB/c mice were plated into 24-well plates at a cell density of 5×10^6 cells/ in DMEM medium supplemented with 10% FBS containing 5 $\mu\text{g/mL}$ of Con A in the absence or presence of different concentrations of **SintMed65** (12, 4 and 1.0 μM) for 48 h. Cells were centrifuged and then pellet washed twice with cold PBS and stained with a solution of PBS with propidium iodide (2 $\mu\text{g/mL}$), RNAase (100 $\mu\text{g/mL}$) and 0.1% v/v of Triton X-100 in the dark at 37 °C for 30 min. The cells were analyzed for cell cycle using flow cytometry (FACS Calibur). A total of 10,000 events were acquired. Cell debris and clumps were gated out, and PreG1, G0/G1, S and G2/M populations were quantified using FlowJo software (Tree Star, Ashland, OR).

4.9. Calcineurin activity

splenocytes from BALB/c mice were plated into 24-well plates at a cell density of 5×10^6 cells/ in DMEM medium supplemented with 10% FBS containing 5 $\mu\text{g/mL}$ of Con A in the absence or presence of different concentrations of **SintMed65** or cyclosporin A (MP Biomedicals, Solon, OH) for 72 h. Then, cells were lysed in a buffer containing protease inhibitors and centrifuged. The same amount of protein (5 μg) per sample was used in the Calcineurin Cellular Activity assay kit (Enzo Life Sciences, Farmingdale, NY, USA), according to the manufacturer's instructions. Colorimetric measurements were performed at 620 nm. The amount of phosphate released by calcineurin was calculated using a standard curve.

4.10. Induction of acute peritonitis in mice

Male BALB/c mice were treated orally with **SintMed65** compound (20 and 80 mg/kg) or vehicle and intraperitoneally with indomethacin (80 mg/kg). After 1 h, animals were challenged with 250 μL injection of carrageenan (1.0 mg/mL). After 4 h, animals were euthanized and peritoneal exudates were harvested by peritoneal lavage using 2 mL of saline solution. Cells were centrifuged at $\times 400\text{ g}$ for 10 min, at 4 °C. The pellet was resuspended in saline (1 mL). Total leukocytes in peritoneal fluid were determined in a Neubauer chamber after dilution in Trypan blue stain. Differential counting of neutrophils was carried out in hematoxylin and eosin-stained cytopspin preparations. A differential count of 200 cells was made in a blinded fashion and according to standard morphologic criteria.

4.11. Statistical analysis

Statistical analysis were performed by one-way analysis of variance and Newman-Keuls multiple comparison tests using Graph Pad Prism version 5.01 (Graph Pad Software, San Diego, CA). Differences were considered significant when the values of P were <0.05 .

Conflict of interest

The authors declared that there is no conflict of interest.

Acknowledgements

This research was funded by Fundação Oswaldo Cruz and Universidade Federal de Pernambuco. C.S.M., C.C.S. and P.S.A. are recipients of CAPES, FAPESB and CNPq scholarships, respectively. D.R.M.M. and M.B.P.S. are recipients of senior fellowships by CNPq (Brazil). We are thankful to the Institute Physics at University of Sao Paulo (Brazil) for allowing the use of diffractometer. The authors are also grateful to Mrs. Daniela Nascimento Silva, Mrs. Eliete de Fátima V. B. N. da Silva, Mrs. Abene Silva Ribeiro and the Analytical Centre of Fundamental Chemistry Department at

Universidade Federal de Pernambuco for the NMR and elemental analysis.

A. Supplementary data

Supplementary data associated with this article can be found, in the online version, at <https://doi.org/10.1016/j.bmc.2018.02.047>.

References

- Kotas ME, Medzhito R. *Cell*. 2015;160:816–827.
- Grivennikov SI, Greten FR, Karin M. *Cell*. 2010;140:883–899.
- Lee M, Rey K, Besler K, Wang C, Choy J. *Results Probl Cell Differ*. 2017;62:181–207.
- Kalinski P. *J Immunol*. 2013;188:21–28.
- Duarte CD, Barreiro EJ, Fraga CA. *Mini Rev Med Chem*. 2007;11:1108–1119.
- Mombelli P, Witschel MC, van Zijl AW, Kaiser Marcel, Illarionova V, Fischer M, Siepe I, Schweizer WB, Brun R, Diederich F, et al. *ChemMedChem*. 2012;7:151–158.
- Carcelli M, Rogolino D, Gatti A, et al. *Sci Rep*. 2016;6:31500.
- dos Santos Filho JM. *Eur J Org Chem*. 2014;29:6411–6417.
- dos Santos Filho JM, Pinheiro SM. *Green Chem*. 2017;19:2212–2224.
- Tributino JLM, Duarte CD, Corrêa RS, et al. *Bioorg Med Chem*. 2009;17:1125–1131.
- Pinheiro PSM, Rodrigues DA, Alves MA, Tinoco LW, Ferreira GB, Sant'Anna CMR, Fraga CAM. *New J Chem*. 2018;42:497–505.
- Maia RC, Tesch R, Fraga CA. *Expert Opin Ther Pat*. 2014;24:1161–1170.
- Gorantla V, Gundla R, Jadaav SS, et al. *New J Chem*. 2017;41:13516–13532.
- Roth HS, Hergenrother PJ. *Curr Med Chem*. 2016;23:201–241.
- Unsal-Tan O, Ozden K, Rauk A, Balkan A. *Eur J Med Chem*. 2010;45:2345–2352.
- de Melo TRF, Chelucci RC, Pires MEL, et al. *Molecules*. 2014;15:5821–5837.
- Montes GC, Hammes N, da Rocha MD, et al. *J Pharmacol Exp Ther*. 2016;358:315–323.
- Kümmerle AE, Schmitt M, Cardozo SVS, et al. *J Med Chem*. 2012;55:7525–7545.
- Abdel-Rahman HM, Abdel-Aziz M, Tinsley HN, Gary BD, Canzoneri JC, Piazza GA. *Arch Pharm Chem Life Sci*. 2016;349:104–111.
- Rodrigues APC, Costa LMM, Santos BLR, et al. *J Enz Inhib Med Chem*. 2012;27:101–109.
- Carvalho SA, Feitosa LO, Soares M, et al. *Eur J Med Chem*. 2012;54:512–521.
- Carvalho SA, Kaiser M, Brun R, da Silva EF, Fraga CA. *Molecules*. 2014;19:20374–20381.
- Song X, Yang Y, Zhao J, Chen Y. *Chem Pharm Bull (Tokyo)*. 2014;62:1110–1118.
- Rodrigues DA, Ferreira-Silva GA, Ferreira AC, et al. *J Med Chem*. 2016;59:655–670.
- Tumer TB, Onder FC, Ipek H, et al. *Int Immunopharm*. 2017;43:129–139.
- Yamamoto Y, Arai J, Hisa T, et al. *Bioorg Med Chem*. 2016;24:3727–3733.
- Lopes AB, Miguez E, Kümmerle AE, Rumjanek VM, Fraga CAM, Barreiro EJ. *Molecules*. 2013;18:11683–11704.
- da Silva TF, Júnior WB, Alexandre-Moreira MS, et al. *Molecules*. 2015;20:3067–3088.
- Rossi A, Pergola C, Koeberle A, et al. *Br J Pharmacol*. 2010;161:555–570.
- Hoozemans JJ, Veerhuis R, Janssen I, Rozemuller AJ, Eikelenboom P. *Exp Gerontol*. 2001;36:559–570.
- Molina-Holgado E, Ortiz S, Molina-Holgado F, Guaza C. *Br J Pharmacol*. 2000;131:152–159.
- Aragoneses-Fenoll L, Montes-Casado M, Ojeda G, et al. *Biochem Pharm*. 2016;106:56–69.
- Azzi JR, Sayegh MH, Mallat SG. *J Immunol*. 2013;191:5785–5791.
- Sheldrick GM. *Acta Cryst*. 2008;A64:112–122.
- Dolomanov OV, Bourhis LJ, Gildea RJ, Howard JAK, Puschmann H. *J Appl Cryst*. 2009;42:339–341.
- Sheldrick GM. *SHELXL97: Program for the Refinement of Crystal Structures*. Germany: University of Gottingen; 1997.
- Green LC, Wagner DA, Glogowski K, Skipper PL, Wishnok JS. *Anal Biochem*. 2009;126:131–138.
- Schmittgen TD, Livak KJ. *Nat Protoc*. 2008;3:1101–1108.